

Fundamental problems in statistical physics XIV: Lecture on Machine Learning

Aurélien Decelle

Departamento de Física, Universidad Complutense, 28040 Madrid, Spain

ARTICLE INFO

Keywords:

Machine Learning
Perceptron
Restricted Boltzmann Machine
Phase Diagram

Abstract


The recent progresses in Machine Learning opened the door to actual applications of learning algorithms but also, to new research directions both in the field of Machine Learning directly and at the edges with other disciplines. The case that interests us is the interface with physics, and more specifically statistical physics. In this short lecture, I will try to present first a brief introduction to Machine Learning from the angle of neural networks. After explaining quickly the based model and the global aspects of the training procedure, I will discuss into more detail two examples to show some interesting developments that can be done from the statistical physics perspective.

1. Introduction

The aim of this lecture and these lecture's notes is to give a basic introduction to Machine Learning and to illustrate by few examples how statistical physics can bring interesting insights and new methods to understand this field. By Machine Learning, I will be more specifically focused on the recent development of neural networks and their applications to classification and generative tasks. I decided to illustrate the work done in statistical physics on simple models that do not need in particular a strong background to understand them and, also, to avoid as much as possible the use of black-box elements that often can make it harder to understand some fundamental aspects of more complex models.

2. Why Machine Learning and Statistical Physics

Statistical physics has traditionally extended its domain of application to other fields than physics only. It is hard, and maybe not useful, to be exhaustive, but looking back into the past, we can already see many contributions in the field of computer science starting in the 80'. At that time, we see the first contributions of statistical physicists to the development and understanding of neural network, such as the Hopfield model[1] or the perceptron[2]. Later on, a lot of work was done in various fields of computer sciences, ranging from constraint satisfaction problems[3] to compressed sensing[4, 5] and more generally bayesian inference[6]. In fact, in the late 90', yet another strong connection between Ising model and bayesian inference was made. It was shown that the so-called Nishimori line[7], a set of coupling constants satisfying a gauge symmetry in a spin glass model, is linked to the bayesian optimal condition in inference problem[8]. Therefore, during the last 30 years, many tools from disordered systems were used, one of the most emblematic being the replica method¹, to study and characterize macroscopic properties of various problems, such as the coloring problem[9], detecting communities[10] or more recently the learning curves of teacher-students neural network[11] or to characterize the phase diagram of unsupervised learning models[12, 13, 14]. Therefore, two approaches can be considered as when speaking on ML and statistical physics. A first approach would consider how ML can be used in concrete applications for statistical physics. For instance, many recent works deal with the use of neural network to classify phase transitions[15], or to cluster the phase space automatically. A second approach, the one which interests us, considers how statistical physics can bring new fundamental questions about ML models and new tools to analyze those. Hence, this lecture focuses on giving the perspective on applying methods or questions from the point of view of a physicist studying ML models.

 adecelle@ucm.es (A. Decelle)

ORCID(s): 0000-0002-3017-0858 (A. Decelle)

¹particularly under the light of the Nobel prize 2021, Giorgio Parisi

3. Basis aspects of Machine Learning

If one would like to be “caricatural”, we can say that ML consists in defining a family of functions and the way to fit its parameters to a given dataset. Said in this simple form seems to be quite reductive, however we should agree that this still implies a lot of aspects to understand. First, how does one define what is a good family of functions and why. Second, how do you fit the parameters. And more profoundly: is there a unique set of good parameters ? and if not, how the learning dynamics, the dynamical process adjusting the parameters to find the good ones, is driven by the dataset? These questions that pop up naturally when first studying the phenomena of adjusting a complicated function to a dataset in order to perform a given task, will, little by little, lead to more profound interrogations such as the geometry of a dataset and of its new (automatically) constructed representation. At some point, we even speak about “semantic representation” when trying to analyze how the transformation performed by ML model can shape a dataset into a set of meaningful categories. In any case, the generic term *latent representation* is typically used to describe the projections that are learned by the models when going through the learning dynamics. To the latent representation are sometimes associated *latent features* to mention the values carried by the weights and it can sometimes be further analyzed. In this lecture, the choice has been taken to first introduce the field of ML starting from basic facts of parameters/curve fitting and progressively explain how to enlarge. However, we do not plan to go further than basics aspects since we need to focus after it to the statistical mechanic approach to the thematic. Before going into more details, let’s discuss first the three broad categories of learning that are classically considered.

3.1. Three categories

Depending on the task and/or the dataset that one consider, three categories of learning methods are usually distinguished.

1. **Supervised Learning:** this formulation indicates that the learning is performed by matching an input \mathbf{x} together with an output value \mathbf{y} , that can be a set of continuous or discrete values. In this setting, the model is trained —the parameters are adjusted— where both the input and output are given.
2. **Unsupervised Learning:** in this formulation, only the set of input is given as entry to the model. The typical case is when the likelihood over a set of samples is maximized. Other options can also be designed, such as *self-supervised learning* where a supervised problem is created out of a generic dataset (with or without label), for instance by masking a part of the data and designing a training where the model should infer the missing values.
3. **Reinforcement Learning:** this case is quite different from the other two, and we will not describe it here. It intends to teach an agent to interact with its environment by means of a Markov decision process. Even though recent successes in IA have shed light on reinforcement learning, see AlphaGo, AlphaStar and AlphaChess, we will not cover this part.

Before entering the details of supervised and unsupervised learning, let’s mention a couple of clear examples for both cases. For the supervised learning, the clearest example is doing a regression. In a regression, you have as input some values \mathbf{x} that correspond to some varying control parameters, and the outputs \mathbf{y} for which the values are known within some error of measurement. In such a case, one needs to choose first a family of functions, typically linear function or polynomials of arbitrary degree. Then, the parameters of the family of function is fitted using the dataset. Here, the coefficient of each term of the polynomial, by typically minimizing the mean square error between the predicted outputs $\hat{\mathbf{y}}$ and the true ones \mathbf{y} . Another example, more typical of the ML field is the task of classification. In that case, the typical family of function used in ML is given by a neural network (the precise form depends on the designed architecture), and the strong difference now is that the output is a category (or an integer).

For unsupervised learning, there are also well-known cases that are generally designed in the Bayesian context. From my point of view, the more famous example is given by the Gaussian mixture model. In this model, the probability density of the dataset is given by a sum of K gaussian distributions. The parameters of all the gaussians is then learned by fitting the likelihood of the probability distribution evaluated on the dataset under consideration. The unsupervised nature of this task relied on the fact that no label is needed — for instance in the case of the mixture of gaussians, the clustering does not depend on the eventually true label of the clusters—.

4. Supervised learning

Let's formalize the problem in the case of supervised learning in order to describe step by step the ingredients of neural networks in that context. We start by considering a dataset $\mathbf{X} \in \mathbb{R}^{N_v \times N_s}$, where N_v is the dimension of the dataset and N_s the number of samples. We then choose a family of functions f_θ , where the dimension of the output depends on the problem considered. For simplicity, let's imagine that we deal with a regression or a binary classification. In that case, the f_θ is one-dimensions and the typical support is \mathbb{R} or $[0, 1]$ respectively.

Regression: we can make the hypothesis that the output is given by the following equation

$$\tilde{y} = \tilde{f}(\mathbf{x}) + \eta \quad (1)$$

where \tilde{f} is the true function relating the input \mathbf{x} to the true output \tilde{y} and η corresponds to some Gaussian noise with zero mean and variance σ^2 . Since we do not know \tilde{f} , we replace it by f_θ and we will now infer θ such that eq. 1 is satisfied. To do that, we can rely on the Bayes theorem:

$$p(\theta | \{\mathbf{x}^{(m)}\}_m, \{\tilde{y}^{(m)}\}_m) \propto p(\{\mathbf{x}^{(m)}\}_m, \{\tilde{y}^{(m)}\}_m | \theta) p(\theta) \quad (2)$$

In the absence of prior $p(\theta)$ on θ , maximizing the left-hand side of eq. 2 corresponds to maximizing the likelihood function $p(\{\mathbf{x}^{(m)}\}_m, \{\tilde{y}^{(m)}\}_m | \theta)$, or equivalently minimizing the inverse of the log-likelihood that is also called the loss:

$$\hat{\theta} = \operatorname{argmin}_\theta [\mathcal{L}(\theta, \{\mathbf{x}^{(m)}\}_m, \{\tilde{y}^{(m)}\}_m)] = \operatorname{argmin}_\theta [-\log(p(\{\mathbf{x}^{(m)}\}_m, \{\tilde{y}^{(m)}\}_m | \theta))] = \operatorname{argmin}_\theta \left[\sum_m \|\tilde{y} - f_\theta(\mathbf{x}^{(m)})\|_2^2 \right]$$

where $\|\cdot\|_2$ correspond to the \mathcal{L}_2 norm. Now, as this expression cannot be minimized easily for any f_θ , a simple way to find $\hat{\theta}$ consists in performing a gradient descent of the loss function \mathcal{L} with respect to the parameters, or weights θ . Writing the gradient descent gives the following learning rules for iterating the values of the parameters θ

$$\theta^{(t+1)} = \theta^{(t)} - \gamma \nabla_\theta \mathcal{L}$$

where γ is the learning rate of the problem. Thus, starting from some initial condition $\theta^{(0)}$, this dynamics tells us how to update the parameters to reach values that should maximize the likelihood. In practice, in ML the gradient descent is slightly modified to take its "stochastic" formulation. What is done is that the gradient is not taken over the whole dataset, but rather on smaller non-overlapping sub-sets called minibatches. Therefore, each update is performed over the gradient computed on a given minibatch, and when all minibatches have been used to update the weights, it is said that it corresponds to an epoch. This dynamics is called Stochastic Gradient Descent (SGD) when using it to minimize a loss. In the context of machine learning, these are somehow the main ingredients at the heart of the learning dynamics. Even though it might seem quite simple, there are many interesting questions about how the learning depends on the shape of f_θ , the number of parameters or even on the initial conditions of these parameters. We will try to approach some of these question in section 8 in a particular context.

Classification: for this task, some precautions need to be taken since the label of the dataset is discrete, as for instance in the case of binary classification $\{0, 1\}$. In fact, we see that by using a family of functions where the output is an integer, the derivative will be zero everywhere, and therefore the gradient descent will give us no information to maximize the likelihood (or to minimize the loss). The generic solution that is considered is to use f_θ that is defined in $[0, 1]$ to describe the probability of being in the class 0 (or 1) instead:

$$p(\mathbf{x}^{(m)} \in C_0) = 1 - f_\theta(\mathbf{x}^{(m)}) \quad \text{and} \quad p(\mathbf{x}^{(m)} \in C_1) = f_\theta(\mathbf{x}^{(m)})$$

From this, we can construct the following likelihood function to maximize. Basically, for each data m , we want to maximize (w.r.t. the parameters θ) its probability to be classified correctly. Therefore, using the true labels $\tilde{y}^{(m)}$ we get

$$p(\{\mathbf{x}^{(m)}\}_m, \{\tilde{y}^{(m)}\}_m | \theta) = \prod_m f_\theta(\mathbf{x}^{(m)})^{\tilde{y}^{(m)}} (1 - f_\theta(\mathbf{x}^{(m)}))^{1 - \tilde{y}^{(m)}}$$

recalling that the outputs $\tilde{y}^{(m)}$ are zero or one. Considering the log-likelihood, we can now define the loss to minimize to be

$$\mathcal{L} = - \sum_m \tilde{y}^{(m)} \log(f_{\theta}(\mathbf{x}^{(m)})) + (1 - \tilde{y}^{(m)}) \log(1 - f_{\theta}(\mathbf{x}^{(m)}))$$

Again, in such a case, the function cannot be minimized directly and a gradient descent is performed, or a learning process, to find the parameters that fit best the likelihood.

4.1. Perceptron: the building block of neural networks

It is now the time to set a simple example, one of the first neural network, called the Perceptron[16]. This example is important for many reasons. First, this model, despite being simple, is a building block of deep neural networks. Therefore, it is interesting to understand its behaviour. Second, its simplicity allows us to understand geometrically how it classifies a dataset. Finally, we can perform two important computations, first we can prove quite easily a useful convergence property. Second, in section 6, we will show how a method from statistical physics allow us to compute the capacity of this model for an artificial dataset.

The perceptron is amongst the first models to use the neural network architecture. Its design is inspired by the neurons of the brains: a neuron is connected to many other neurons. It can fire (be in an excited state) if it received a sufficient number of exciting signal from neurons connected to it, and otherwise it stays at rest. The way it was formalized is as follows. We consider a neuron y connected to a set of N_v neurons $\{x_i\}$. The neuron will be activated with the following the rule:

$$y(\mathbf{x}) = \text{sgn}\left(\sum_{i=1}^{N_v} x_i w_i - \alpha\right) \text{ with } \text{sgn}(x) = \begin{cases} 1 & \text{if } x \geq 0 \\ -1 & \text{if } x < 0 \end{cases} \quad (3)$$

It is common to illustrate this type of model using the picture on the left panel of fig. 1. We see that in order to activate the neuron y , the input signal \mathbf{x} pondered by the weights \mathbf{w} should be higher than the threshold α , otherwise it remains inactivated. Now, we should understand that a neuron is excited if the input is matching a given pattern that is being recognized. We can thus classify an input according to the excitation state of the output neuron. For instance, let's imagine that we want to distinguish two classes of objects. We wish to find the parameters \mathbf{w} such that for a given class the output is always 1 while for the other class the output is always -1 . We recognize here the same spirit as for regression tasks: adjusting the weight to obtain a given output. What makes precisely the perceptron a neural network is the choice of the family of functions. In practice, the term neural network is used for families of functions where the output corresponds to a linear operation of the inputs, eventually followed by a non-linearity. In this case, the non-linearity is given by the sign function, but we will see later that more clever choices can be made.

Before defining the learning rules of the binary perceptron, we can analyze quickly the geometry of the obtained model. We see that, the decision boundary (the set of vectors \mathbf{x} which are exactly at the border between two classes) corresponds to the solution of the following equation

$$\sum_{i=0}^{N_v} x_i w_i = 0 \iff \mathbf{x} \cdot \mathbf{w} = 0$$

where we used the notation $x_0 = 1$ and $w_0 = -\alpha$. We recognize the equation of a hyperplane of dimension $N_v - 1$. Hence, the perceptron cuts the N_v -dimensional space into two separate parts, where on one side the output is 1 and on the other side it is -1 . From this property, we can already identify a limitation of this model: in order to be able to classify correctly a whole dataset, the representation of the data in the N_v dimensional space should be linearly separable — there should exist a hyperplane that separates the two classes. See right panel of fig. 1 for an illustration in two-dimension.

Learning Rule: in general, the learning rule is derived from the gradient of a loss function. The loss function is often written in terms of some likelihood function or by the classification error. However, in this toy model, the classification is a piece-wise constant function and therefore the gradient is zero almost everywhere. Still, a loss function can be designed for misclassified datapoints. When dealing with a misclassified datapoint, we take as loss the distance between

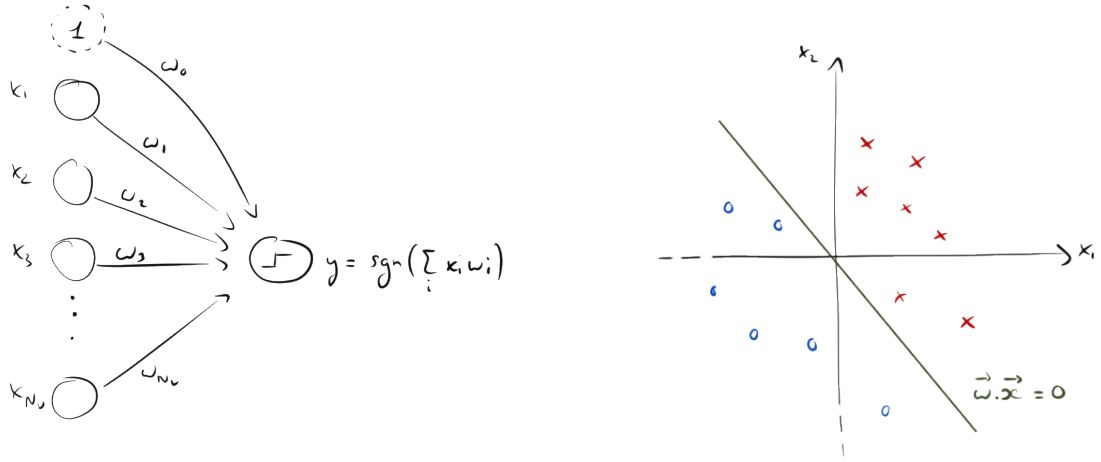


Figure 1: **Left:** illustration of the Perceptron. The nodes on the left represent the input and the bias. The output is defined by taking the sign of the scalar product of the input and the weights. **Right:** Illustration of a “classifiable” dataset, with the solution separating the two groups of data

the point and the decision boundary (see [17] for more details). In that case, using the oriented distance, we can write for a given datapoint m :

$$E(\mathbf{x}^{(m)}) = \tilde{y}^{(m)} \frac{\mathbf{x}^{(m)} \cdot \mathbf{w}}{\|\mathbf{w}\|}$$

Since the denominator is only a multiplicative factor depending on the norm of \mathbf{w} , we can discard it and consider the following gradient

$$\nabla_{\mathbf{w}} E(\mathbf{x}^{(m)}) = \tilde{y}^{(m)} \mathbf{x}^{(m)}$$

giving the learning dynamics for the datapoint (m)

$$\mathbf{w}^{(t+1)} = \mathbf{w}^{(t)} + \gamma \mathbf{x}^{(m)}$$

where γ is the learning rate. Hence, we can write the learning algorithm for the perceptron

Algorithm 1 Learning algorithm for the binary perceptron

Input: Data: $\mathbf{X} \in \mathbb{R}^{N_v \times N_s}$, Labels: $\tilde{\mathbf{Y}} \in \{-1, 1\}^{N_s}$, Weights: $\mathbf{w}^{(0)}$, learning rate $\gamma = 1$, t_{\max}

Output: $\mathbf{w}^{(*)}$.

ϵ = Nb of misclassified datapoints.

$T = 0$

while $\epsilon \geq 0$ and $t_{\max} \geq T$ **do**

for $m = 0 \rightarrow M$ **do**

 Compute $c = \tilde{y}^{(m)}(\mathbf{x}^{(m)} \cdot \mathbf{w})$ — negative for misclassified data

if $c \leq 0$ **then**

$\mathbf{w}^{(t+1)} = \mathbf{w}^{(t)} + \gamma \tilde{y}^{(m)} \mathbf{x}^{(m)}$

end if

end for

$T = T + 1$

end while

return $\mathbf{w}^{(*)} = \mathbf{w}^{(T_{\text{final}})}$

Interestingly, it can be proved rigorously that this algorithm converges whenever the data are linearly separable. However, the proof does not tell you how long you need to wait!² This closes the section on the (historical) binary perceptron. In the following, we will see a more classical view of multiclass/multilayers perceptron and where the loss function is defined as a likelihood using a Bayesian approach and where the gradient is naturally given by the derivative of the likelihood of the model.

4.2. Multilayer perceptron

Let's first consider the case of a multiclass perceptron using a Bayesian approach, and later we introduce the possibility to have many hidden layers. It is much more convenient to deal with a probabilistic approach to the perceptron. It can be written easily for an arbitrary number of classes, and the loss to be minimized can be cast as a maximum likelihood formulation. Also, each datapoint will be assigned a probability to belong to a cluster instead of a hard assignment. In this formulation, instead of having one output, we have K of them. Therefore, we will note the output y_a and \mathbf{w}_a the associated set of weights for the neuron a . The true label of the dataset will be now a *one hot vector*: if the data m is in class $\tilde{y} \in \{0, \dots, K-1\}$, we build the vector $\tilde{\mathbf{y}}$ which has all components to zero except the one corresponding to its class, which is put to one. For instance, if the data m is in the class b , we will define its label as $\tilde{y}_a^{(m)} = 0$ for $a \neq b$ and $\tilde{y}_b^{(m)} = 1$. In particular, we have that $\sum_a \tilde{y}_a^{(m)} = 1$. Now, we define the K outputs of the multilayer perceptron $y_a(\mathbf{x})$. They are given by a *softmax* activation function:

$$y_a(\mathbf{x}) = \frac{\exp(\mathbf{x} \cdot \mathbf{w}_a)}{\sum_{c=0}^{K-1} \exp(\mathbf{x} \cdot \mathbf{w}_c)} = \frac{\exp(\sum_i x_i w_{ia})}{\sum_{c=0}^{K-1} \exp(\sum_i x_i w_{ic})}$$

We see that the output is normalized such that can be interpreted as a probability distribution: they are all positive and sum to one. We can also remark that, the ratio of probability between two classes is

$$\frac{y_a(\mathbf{x})}{y_b(\mathbf{x})} = \frac{\exp(\mathbf{x} \cdot \mathbf{w}_a)}{\exp(\mathbf{x} \cdot \mathbf{w}_b)} = \exp(\mathbf{x} \cdot (\mathbf{w}_a - \mathbf{w}_b))$$

Again, for a given weight matrix \mathbf{w} , the separation between two classes is given by a hyperplane, this time the equation is $\mathbf{x} \cdot (\mathbf{w}_a - \mathbf{w}_b) = 0$. More precisely, we can demonstrate that any pair of points within a given class, can be linearly interpolated by other point still belonging to the same class.

Once the model is defined, we should decide the loss function that we want to minimize. In this case, we can easily define a likelihood over the model. As for the binary perceptron, we want to maximize the probability that a data is correctly classified, and maximize it with respect to the model's parameters. The probability that the data \mathbf{x} is correctly classified according to its label \tilde{y} (or equivalently its one-hot vector $\tilde{\mathbf{y}}$) is

$$p(\mathbf{x} \in C_{\tilde{y}} | \mathbf{w}) = y_{\tilde{y}}(\mathbf{x}) = \prod_a y_a(\mathbf{x})^{\tilde{y}_a}$$

Taking the log, we obtain the following function to maximize

$$\mathcal{L} = \sum_m \left[\sum_a \tilde{y}_a^{(m)} \log(y_a(\mathbf{x}^{(m)})) \right]$$

This function is also coined as : binary cross-entropy (in the case of two classes) and categorical cross-entropy in the most general case. To maximize the log-likelihood we rely again on the gradient ascent dynamics. The gradient can be easily computed

$$\frac{\partial \mathcal{L}}{\partial w_{ia}} = x_i [\tilde{y}_a - y_a(\mathbf{x})]$$

and the learning dynamics hence follow the iterative process

$$w_{ia}^{(t+1)} = w_{ia}^{(t)} - \eta x_i [\tilde{y}_a - y_a(\mathbf{x})]$$

²An upper bound is given on the number of updates assuming some hypothesis on the margin that separates the two classes. However, we do not know this margin in general.

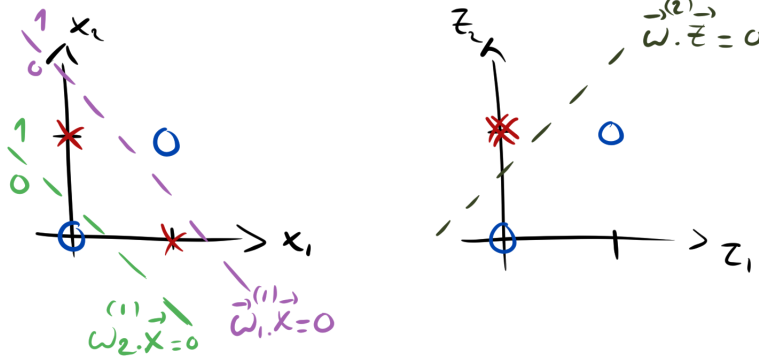


Figure 2: The mechanism of the multilayer perceptron. On the left, we show the XOR dataset in blue and red, which is clearly non-separable by a single hyperplane. In purple and green, the decision surface of the associated to the two hidden nodes respectively. We give the latent code for given by each half-plane associated with the hidden nodes. On the right, the projection on in the hidden space of the dataset given by the latent encoding and a potential decision surface.

Towards multilayer: we saw that the perceptron with only one input layer connected directly to the output neurons is not capable to classify correctly the dataset that are not linearly separable. To overcome this limitation, we will see how the introduction of a hidden layer can solve the problem in a simple example. However, even if we can construct a solution in a simple example, we have no guarantee that the gradient ascent dynamics would converge to it.

Let's consider the following dataset:

$$\left\{ \begin{array}{l} \mathbf{x}^{(1)} = \begin{pmatrix} 0 \\ 0 \end{pmatrix} \\ \tilde{y}^{(1)} = 0 \end{array} \right\}, \left\{ \begin{array}{l} \mathbf{x}^{(2)} = \begin{pmatrix} 1 \\ 1 \end{pmatrix} \\ \tilde{y}^{(2)} = 0 \end{array} \right\}, \left\{ \begin{array}{l} \mathbf{x}^{(3)} = \begin{pmatrix} 1 \\ 0 \end{pmatrix} \\ \tilde{y}^{(3)} = 1 \end{array} \right\}, \left\{ \begin{array}{l} \mathbf{x}^{(4)} = \begin{pmatrix} 0 \\ 1 \end{pmatrix} \\ \tilde{y}^{(4)} = -1 \end{array} \right\} \quad (4)$$

which correspond to the XOR function. It is clear that this dataset cannot be classified correctly by the perceptron since it is not linearly separable, see on fig 2 left panel. We consider now this simple multilayer perceptron. We have two variables x_1, x_2 as input. Then a set of two hidden neurons z_1 and z_2 connected to \mathbf{x} by a set of weight $\mathbf{w}^{(1)}$ and finally an output neuron y connected to \mathbf{z} by a set of weight $\mathbf{w}^{(2)}$. We define now the relation between these variables:

$$\begin{aligned} z_1 &= \text{sig}(\mathbf{w}_1^{(1)} \cdot \mathbf{x}) \\ z_2 &= \text{sig}(\mathbf{w}_2^{(1)} \cdot \mathbf{x}) \\ y &= \text{sig}(\mathbf{w}^{(2)} \cdot \mathbf{z}) \end{aligned}$$

again we considered that the zero component of \mathbf{x} and \mathbf{z} is 1 to take into account the biases, and $\text{sig}(x) = (1 + e^{-x})^{-1}$ is the sigmoid function. We can interpret the first layer as the composition of two "simple" perceptrons. In this interpretation, the first hidden layer will cut the input space by two hyperplanes (here lines). Each of the four sub-parts of the plan will then be projected onto another 2-dimensional space with latent code 00, 01, 10 and 11. The whole game now is to find the parameters for the two perceptrons $\mathbf{w}_1^{(1)}$ and $\mathbf{w}_2^{(1)}$ such that the latent code of the dataset is linearly separable in the latent space of the variable \mathbf{z} . Then, the last perceptron $\mathbf{w}^{(2)}$ will be able to classify correctly the dataset. This achieves to explain how a multilayer perceptron can overcome the problem of separability of the dataset, and we can see empirically that the gradient descent do converge in this toy example. See on fig. 2 an illustration of this phenomena.

4.2.1. Multilayer perceptron

For the sake of completeness, we will derive here the so-called back-propagation algorithm that is used to compute the gradient efficiently. Back-propagation (or chain-rule) is one of the reasons why neural network can be used in

practice, since it allows the computation of the gradient very quickly and to be optimized by linear algebra and parallel operations. Let's deal with the case of one hidden layer, since adding more layers is just as easy but more cumbersome to write. The model of the multilayer perceptron with one hidden layer is designed as follows. We still start from a set of N_v input nodes. Then we add a hidden layer of N_h neurons. Each neuron of the hidden layer will be a linear function composed with a non-linearity, also called an activation function. We finally have an output layer made of K neurons associated with a softmax activation function.

Let's note \mathbf{x} the input vector, \mathbf{z} the hidden nodes, \mathbf{y} the output layer and $\mathbf{w}^{(1)}$, $\mathbf{w}^{(2)}$ the weights between the input layer and the first hidden layer, and the weights between the hidden nodes and the output layer respectively, as can be seen on fig. 3 left panel. The hidden nodes are given by

$$z_0 = 1$$

$$z_\alpha(\mathbf{x}) = f_1(\mathbf{x} \cdot \mathbf{w}_\alpha^{(1)}) \quad \alpha = 1, \dots, N_h$$

where f_1 is the activation function. The outputs are given by

$$y_a(\mathbf{z}) = \frac{\exp(\mathbf{z} \cdot \mathbf{w}_a^{(2)})}{\sum_{c=1}^K \exp(\mathbf{z} \cdot \mathbf{w}_c^{(2)})}.$$

The typical activation functions are the sigmoid or the Rectified Linear function:

$$\text{ReLU}(x) = \begin{cases} x & \text{if } x \geq 0 \\ 0 & \text{if } x < 0 \end{cases} \quad (5)$$

The likelihood of the model is then

$$\mathcal{L} = \sum_m \left[\sum_a \tilde{y}_a^{(m)} \log(y_a(\mathbf{z}(\mathbf{x}^{(m)}))) \right]$$

We can now show how to compute the gradient using the chain rule. First, we see that the gradient w.r.t. the $\mathbf{w}^{(2)}$ gives the same expression as for the multiclass perceptron where the input is changed for the variable of the hidden layer:

$$\frac{\partial \mathcal{L}}{\partial w_{ab}^{(2)}} = z_a [\tilde{y}_b - y_b(\mathbf{z})] = z_a \delta_b^y$$

where we define the variables $\delta_b^y = \tilde{y}_b - y_b(\mathbf{z})$. A more complicated task is to compute the gradient w.r.t. the weights $\mathbf{w}^{(1)}$. This can be done without suffering too much using the derivative chain rule.

$$\begin{aligned} \frac{\partial \mathcal{L}}{\partial w_{ia}^{(1)}} &= \sum_a \tilde{y}_a \frac{\partial y_a}{y_a} \frac{\partial y_a}{\partial w_{ia}^{(1)}} \\ \frac{\partial y_a}{\partial w_{ia}^{(1)}} &= \sum_\beta \frac{\partial z_\beta}{\partial w_{ia}^{(1)}} \frac{\partial y_a}{\partial z_\beta} \quad \text{with} \quad \frac{\partial y_a}{\partial z_\beta} = y_a w_{a\beta}^{(2)} - y_a \sum_c w_{c\beta}^{(2)} y_c \\ \frac{\partial z_\beta}{\partial w_{ia}^{(1)}} &= x_i f'_1(\mathbf{x} \cdot \mathbf{w}_\beta^{(1)}) \delta_{\alpha\beta} \end{aligned}$$

From this we can obtain the gradient as a matrix-vector product using the variables δ^y defined previously

$$\frac{\partial \mathcal{L}}{\partial w_{ia}^{(1)}} = x_i f'_1(\mathbf{x} \cdot \mathbf{w}_a^{(1)}) \sum_a w_{aa} \delta_a^y$$

This mechanism remains true for deeper network: we can write the gradient deep in the network as a matrix-vector product between the previously computed gradient and the weight corresponding at the next layer. Hence, the structure of the gradient enable the possibility to compute it very quickly in computer time, and therefore making these network

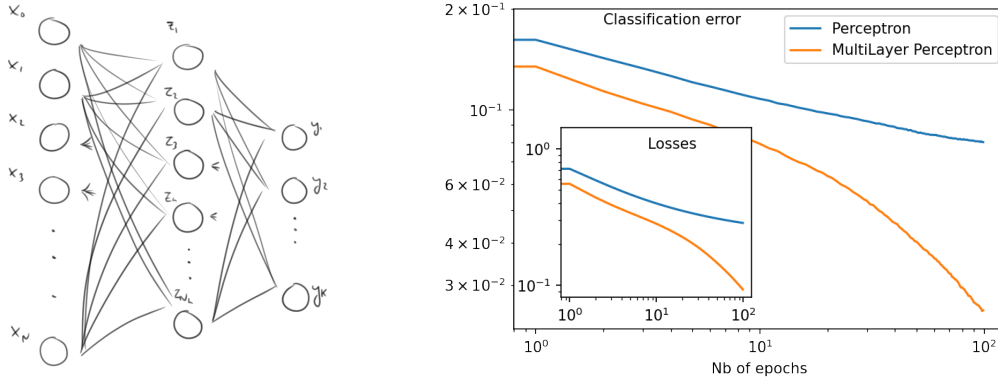


Figure 3: Left: A schematic view of the multilayer (with one hidden layer) perceptron. Right: Learning curve (loss function and classification error) of the perceptron and of the multilayer perceptron with one hidden layer of $N_h = 100$ nodes.

trainable in practice. This method has been called “back-propagation” where it is understood that the error is back-propagated deeper in the network, even though there is nothing more than the chain rule.

We show on figs 3 right panel an example of training for two cases. In the first one, we take a simple perceptron without hidden layer. In the second case, we take a hidden layer of $N_h = 100$ hidden nodes and again show the behavior of the loss function (inverse of the log-likelihood) and of the classification error: for a data \mathbf{x} , the data is said to be classified correctly if the output with the highest value (or highest probability) of the perceptron corresponds to the correct class. We see that the extra hidden layer is improving substantially the performance, both looking at the accuracy and of the loss.

4.3. Regression

Regression can be dealt with as easily as the classification task. The most notable difference is that the target is usually a continuous value rather than a categorical variable. In this situation, it is enough to adjust the activation function of the last layer of the neural network. A common choice is to use the identity as an activation function such that the output can be mapped into \mathbb{R}^K where K is the dimension of the output. There is no need to enter into more details concerning the computation of the gradient and the learning dynamics since most part is covered already in the previous section. We will take advantage of the regression case to illustrate briefly the fitting properties of neural network in that case. It can be shown that neural network with one arbitrarily large hidden layer are “universal approximators”. This is to say that it can fit arbitrarily well any function, as is the case for the polynomials. To understand this, let’s consider a simple example. We imagine that the curve we want to fit is from \mathbb{R} to \mathbb{R} . Now, let’s imagine that we want to approximate our function g defined within x_m and x_M by a piece-wise constant function. Let’s indicate the abscissa at which each continuous pieces starts as x_i , with $i = 1, \dots, N_h$ and let’s take for simplicity $x_{i+1} - x_i = \delta$. For each x_i , we will associate the value $\hat{y}_i = (g(x_i) + g(x_{i+1}))/2$, see fig. 4 left panel for an illustration. Using this construction, we see that by increasing the number of pieces, the approximation is getting better and better. Now, we can construct explicitly a neural network giving such an output. Let’s consider a neural network with one input, one output and a hidden layer of N_h hidden nodes. For the first hidden node, we can fix the weight to one and the bias to $-x_m$: $w_{11}^{(1)} = 1$ and $w_{01}^{(1)} = -x_m$. In this way, the neuron will activate as soon as the input pass the value x_m . Then, the weight between this node and the output can be fixed at $w_1^{(2)} = \hat{y}_0$ such that it reproduces the first piece of the piece-wise continuous approximation. Then, for the second neuron, we repeat the same operation but, putting the bias to $w_{02}^{(1)} = -x_m - \delta = -x_1$. Then the weight with the output node will be set to $-\hat{y}_0 + \hat{y}_1$ in order to take into account the first activated nodes. Now, it is clear that following this construction, we will reproduce the piece-wise continuous approximation defined above with our neural network. As stated before, the approximation can be made arbitrarily good by taking higher values of N_h which therefore show that a one-hidden layer neural network can approximate any function, we give a quick example of the results obtained in a simple case explained below and on fig. 4 right panel. The same is true for classification, and neural networks are therefore universal approximators.

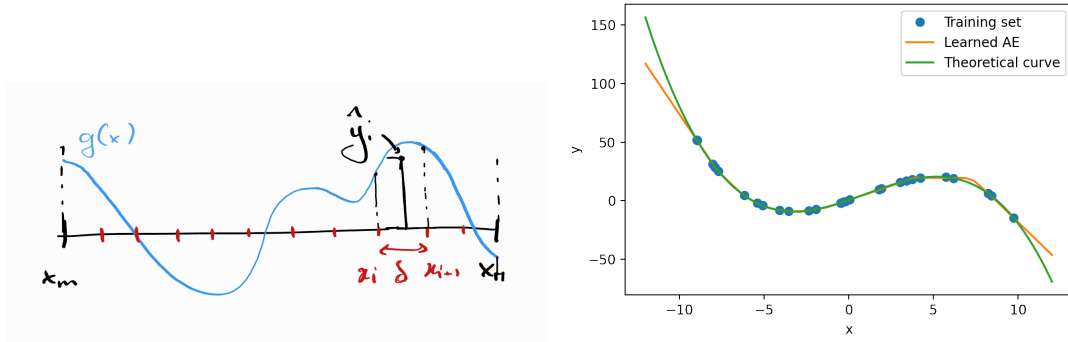


Figure 4: **Left:** an illustration of the discretization process that is used to encode directly a solution to the neural network. **Right:** we see the result of the training of a neural network with $N_h = 30$ nodes to regress a polynomial. The neural network fits very well the training points, and is quite good at reproducing the trend of the function in this range. As soon as we take values of x outside of the training dataset range, the result diverges quickly with the theoretical function as expected.

As an example, we show below the result of a feed-forward neural-network applied to a simple polynomials curve. For this, we use a multilayer neural network associated to a regression task, where the input and output are of dimension one, and that has one hidden layer of dimension N_h . The training of the machine is done using a Stochastic Gradient Descent algorithm and the cost function is simply given by the ℓ_2 norm. In practice, we therefore have the following function for the output of the hidden layer and the output:

$$z_\alpha(x) = f_1(w_{\alpha 0}^{(1)} + xw_{\alpha 1}^{(1)}) \quad (6)$$

$$y(z) = \sum_{\alpha} z_{\alpha} w_{\alpha}^{(2)} \quad (7)$$

where f_1 is the activation function for the first layer, here we take $f_1(x) = \text{ReLU}(x) = \max(0, x)$ and the second layer is a linear combination of the hidden entries. Using this simple model, we show below the result of a training with $N_h = 30$, see fig. 4 right panel.

4.4. Some works on generalization

Up to now, we only focused on the learning properties of some models according to a set of data on which the parameters are fitted. However, often the “true” goal of Machine Learning is that the learned model can be applied to other data, that were not previously included in the one used for training. It is also quite important because we do not wish that our model overfits the training data, as can occur quite easily when the number of parameters of the models is higher than the number of training samples. Without entering into detail, we will just remind the definition of the training error and the generalization error for practitioners. They are concepts to which we will come back to later on.

In practice, one starts with a dataset X , having N_s samples. In order to evaluate a learned model and to check for overfitting, the dataset is cut into two pieces. A set of N_{training} samples will be used for training, defining the training set. Then, another set of N_{test} samples, called the test set, is used for measuring performance on unseen samples. Usually, something around 80% to 90% of all samples are used for training and the rest for the test. The typical practice is to train the model on the training set, and to evaluate its performance on the test set. In some more complex case, one has also to fix some meta-parameters of the model such as the time at which the training is stopped, the value of some regularization etc. In that case, an additional set, the validation set, is used to fix the optimal value of the meta-parameters and then the model is tested on the test set. This procedure is obviously not perfect but allows defining a clear protocol to compare model. In section 6 we will see how the definitions are extended in the case where we have a generative model for the dataset.

4.5. Deep-Learning and Convolutional Neural Network

To end up with supervised learning, I just want to describe briefly an important piece of deep-learning: the convolutional neural network or CNN[18]. The CNN has been introduced to deal with translational invariance,

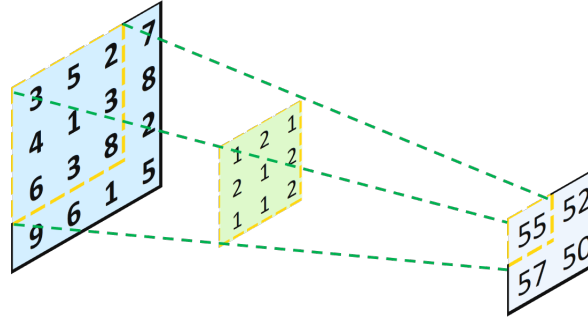


Figure 5: Illustration of a CNN with 3×3 kernel

particularly for image dataset. In practice, one would like that the features learned by the neural network do not depend on the precise location where it has been detected. A very heavy way to implement this translational invariance, would be to add to the dataset every possible translation of it and to train the neural network with this augmented dataset. A simpler way to achieve this is by using CNN. Let's describe it for the case of images. A CNN consists of a perceptron with a small number of input nodes and that take into consideration the geometry of the input. Let's take the example where inputs are images. We consider a small perceptron having the shape of 5×5 nodes, thus square shaped. The perceptron will be "applied" to the whole image by the following procedure. The square shaped perceptron will take as input sub-part of 5 pixels of the images and compute the output value. Then, the pixels used as input will be changed, by "moving" the perceptron from left to right, up to bottom on the image, spanning it completely and producing an output for each different set of inputs. The important point here, is that all the output are made using the same set of weights associated to the CNN, see fig. 5 for an illustration. In other words, if we consider the CNN as the following function

$$f_{\text{CNN}}(x, y) = \begin{cases} w_{xy} & \text{if } |x| \leq 5 \text{ and } |y| \leq 5 \\ 0 & \text{otherwise} \end{cases}$$

The number of parameters for this plaque is therefore 5×5 to which we add the bias. Then, the output given by the CNN applied to the image is

$$z(x, y) = f_1 \left(\int dx' dy' f_{\text{CNN}}(x - x', y - y') \text{input}(x', y') + b_{xy} \right)$$

where f_1 is an activation function and b_{xy} the bias. The CNN are usually pictured as on fig. 5. In general, there is an extra parameter corresponding to the number of pixels the kernel or plaque is moved during the convolution. Its default value is often one, but it is possible to shift the kernel using larger values. Depending on the boundary condition, we can either have an output of the same dimension as the input, or slightly reduced depending on the sliding parameter defined previously, hence reducing the overall dimension. To a given plaque, we hope that the neural network will learn a particular filter relevant for the task we are considering. In general, one layer of CNN is considered to be defined by many plaques, since we want to detect many different features. Therefore, we will typically have a set of neurons in the CNN-layer to scale as $S_x \times S_y \times N_p$ where N_p is the set of used plaques.

In practice, the convolutional layer is put together with a 'MaxPooling' layer which is further reducing the output to avoid overfitting, but it is out of range of this lecture to start describing the whole set of possible tricks to train a neural network. In general, it is common to stack many CNN, with possible different shapes to build the architecture. Before going to the output layer, it is useful to add a fully-connected layer that will make use of the learned features of the CNN to classify the dataset.

This concludes this introduction to supervised learning, using simple block of neural network.

5. Unsupervised learning

In the unsupervised learning formalism, the setting is different from the supervised case for the fact that we do not have a target or label variable associate to each data. In that setting, the general goal is to find a model that reproduces the

dataset density distribution in some sense. In this section, we will quickly revise the classical models of unsupervised learning based up on a neural networks' architecture.

5.1. Auto-Encoder

We begin with a simple model, the AutoEncoder (AE), which is a simple way to construct an unsupervised model using neural networks. We will not enter into too much detail of the AE but rather explain its design. As explained before, in the unsupervised learning context, the dataset does not contain any label. Yet, it is possible to construct a simple NN without any need for a label. The AE consists in, starting from an input, to perform a set of transformations, starting from the dataset and generating as output a vector of the same dimension. We will adjust the parameters of these transformations such that the output is as close as possible to the input. Therefore, defining the input \mathbf{x} , a function $\mathbf{y} = \mathbf{f}_\theta(\mathbf{x})$ which has the same dimension as the input. In the context of a neural network, the design of \mathbf{f}_θ is typically made of hidden layers such as the ones defined in the supervised section, and convolutional layers. Each hidden layer has its own activation function and for the last layer, the dimension of the output is fixed to be the same as the one of the input while the activation should be adjusted to cover the space in which the dataset is defined. For instance, when dealing with a dataset in $[0, 1]$, the last activation function is the sigmoid and the loss being the cross-entropy between the input and the output. In the case where the input lives in \mathbb{R} , the activation function is the identity and the loss is often the ℓ_2 norm between the input and the output. As a matter of fact, the AE can be seen as a regressive neural network, where the output nodes are the same ones as the input. With this in mind, one can convince himself that having understood the section on regression is enough to understand the learning mechanism of the AE.

The AE is often seen as a machine able to learn a meaningful and compressed representation of the data [19, 20]. As such, the set of layers chosen in many cases is first operating a reduction of the number of nodes at each layer, and then a set of layer taking the low-dimensional input and bringing it to the same dimension as the dataset's input. The first part is usually referred as to the "encoder" while the second one is the "decoder".

Practical uses of AEs are less clear in comparison to classifiers. To cite few examples, it can be used to for instance automatically find a hopefully meaningful representation of the dataset, that can sometimes be used for classification task later on. Also, it can be trained to performed denoising task[21]: giving as input a noisy version of a data but asking the output to be as close as possible of the denoised version. It can then perform a denoising task on new data. Finally, it is the basis of the variational AE that we will briefly mention in a subsequent section.

5.1.1. Variational Auto-Encoder

A few words on Variational Auto-Encoder (VAE). VAE is a clever construction to design latent-variable generative model. A latent variables model consists in defining a set of latent variables \mathbf{z} associated to a simple prior distribution $p(\mathbf{z})$. And to define the following posterior distribution over the space of the data

$$p_\theta(\mathbf{x}) = \int d\mathbf{z} p_\theta(\mathbf{x}|\mathbf{z})p(\mathbf{z})$$

where we need to specify $p_\theta(\mathbf{x}|\mathbf{z})$. A classical approach, is to use a neural network to define the conditional distribution as

$$p_\theta(\mathbf{x}|\mathbf{z}) = \mathcal{N}(\mathbf{x}|\mathbf{f}_\theta(\mathbf{z}), \sigma)$$

where \mathcal{N} is the Gaussian distribution and $\mathbf{f}_\theta(\mathbf{z})$ a neural network taking \mathbf{z} as input and depending on a set of parameters θ . However, in many cases, the posterior distribution $p_\theta(\mathbf{x})$ is intractable. Using variational approaches, VAE finds a way to maximize approximately the likelihood. First, let's observe that if the likelihood is intractable, so is the conditional probability $p_\theta(\mathbf{z}|\mathbf{x})$ since it is directly related to $p_\theta(\mathbf{x})$ by the Bayes theorem. This would be a problem if we wanted to use expectation-maximization³ approach as is the case of the mixture of Gaussian models. So instead, we will introduce a simpler function $q_\lambda(\mathbf{z}|\mathbf{x})$ to approximate $p_\theta(\mathbf{z}|\mathbf{x})$ which depends on some parameters λ . Now let's write the likelihood of the model

$$\log p_\theta(\mathbf{x}) = \mathbb{E}_q[\log p_\theta] = \mathbb{E}_q \left[\log \left(\frac{p_\theta(\mathbf{x}, \mathbf{z})}{p_\theta(\mathbf{z}|\mathbf{x})} \frac{q_\lambda(\mathbf{z}|\mathbf{x})}{q_\lambda(\mathbf{z}|\mathbf{x})} \right) \right] = \mathbb{E}_q \left[\log \left(\frac{p_\theta(\mathbf{x}, \mathbf{z})}{q_\lambda(\mathbf{z}|\mathbf{x})} \right) \right] + \mathbb{E}_q \left[\log \left(\frac{q_\lambda(\mathbf{z}|\mathbf{x})}{p_\theta(\mathbf{z}|\mathbf{x})} \right) \right]$$

³for more details see the wikipedia page of EM.

where $\mathbb{E}_q[\cdot]$ represent the average with respect to the distribution q_λ . The second term correspond to the Kullback-Leibler (KL) divergence between our “simple” distribution q_λ and the conditional distribution of \mathbf{z} . By definition, it is always positive, and zero if both are equal. Therefore we can rewrite this equation as

$$\mathbb{E}_q \left[\log \left(\frac{p_\theta(\mathbf{x}, \mathbf{z})}{q_\lambda(\mathbf{z}|\mathbf{x})} \right) \right] = \log p_\theta(\mathbf{x}) - D_{KL}[q_\lambda(\mathbf{z}|\mathbf{x}) || p_\theta(\mathbf{z}|\mathbf{x})] \quad (8)$$

And we see that by maximizing the left hand side of eq. 8 with respect to all the parameters of the problem: $\{\theta, \lambda\}$, we are at the same time increasing the likelihood of our distribution and decreasing the KL divergence between the true posterior $p_\theta(\mathbf{z}|\mathbf{x})$ and q_λ . So far, we understand why all this is “variational” aspect, but the AE part is not clear. The reason is that, we will interpret $q_\lambda(\mathbf{z}|\mathbf{x})$ to be somehow the encoder part of the AE, transforming an input \mathbf{x} into its latent representation \mathbf{z} . While the decoding part is represented by $p_\theta(\mathbf{x}|\mathbf{z})$, transforming a latent representation \mathbf{z} into the data-space. More information on practical details and implementation can be found here[22, 23, 24].

5.2. Restricted Boltzmann Machine

The Restricted Boltzmann Machine (RBM) is a very appealing model for statistical physicist as it can be seen as a bipartite Ising model. Its architecture is very similar to simple AE, however the training procedure is very different, as we will see quickly. First, the RBM is a probabilistic model defined on the space where live the dataset, and a set of hidden nodes. The usual goal when dealing with RBM is to learn the empirical data distribution within a simple analytical formulation, with the hope that we will be able to generate new data statistically similar as the ones of the dataset (but obviously different from it). The training procedure is based on the maximization of the likelihood of our probabilistic model evaluated on the dataset.

Let’s define the model. First, we need to define the input space, corresponding for the RBM to the visible nodes: s_i with $i = 1, \dots, N_v$ and the set of hidden nodes τ_μ , with $\mu = 1, \dots, N_h$. Then, we define the following Hamiltonian

$$\mathcal{H}[\mathbf{s}, \boldsymbol{\tau}] = - \sum_{i,\mu} s_i w_{i\mu} \tau_\mu - \sum_i s_i \theta_i - \sum_\mu \tau_\mu \eta_\mu \quad (9)$$

where classically, the visible and the hidden nodes are binary discrete variables $\{0, 1\}$. The weight matrix \mathbf{w} represents the couplings between the visible and the hidden nodes, while the parameters $\boldsymbol{\theta}$ and $\boldsymbol{\eta}$ are local biases. In practice, any prior distribution can be taken for the visible and the hidden nodes. For instance, the choice of binary $\{\pm 1\}$ is completely equivalent to the previous choice, but it is also possible to consider categorical variables, or even continuous ones using the Gaussian distribution. We note that, if taking a Gaussian prior for the hidden nodes, the distribution over the visible nodes can be mapped to the one of a Hopfield model, see appendix 10.3. This Hamiltonian describes a bi-partite Ising model where interactions are present only between the visible and hidden nodes, but are absent within each layer, see fig. 6.

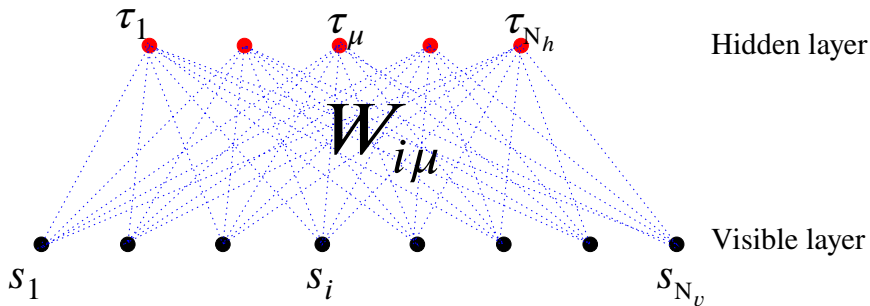


Figure 6: bipartite structure of the RBM.

The idea behind the RBM is that, the correlations between the visible nodes, which should correspond to the correlation of the dataset, will be captured by the interactions between the visible and the hidden layer. This is somehow

a different approach from the one of the Boltzmann Machine where interactions between visible nodes are present and should modelize the true network architecture. Looking at the marginal distribution over the visible nodes:

$$p(s) = \sum_{\tau} p(s, \tau) = \frac{1}{Z} \exp \left(\sum_i s_i \theta_i + \sum_{\mu} \log[1 + \exp(\sum_i w_{i\mu} s_i + \eta_{\mu})] \right) \quad (10)$$

It is easy to see that this distribution include potentially interactions between the visible nodes at all possible order, for instance by making an expansion of the log. This means that a RBM having discrete variables for the hidden layer can describe a system with higher (than-two) order interactions without the need of specifying exactly which ones.

The popularity of this model, both for the field of Machine Learning and for physicists, came for its ability to learn the empirical density of complex datasets. The learning procedure based on the maximum likelihood approach is described into more details in section 8.

5.3. Generative Adversarial Network

Generative Adversarial Network[25] (or GAN) is a generative model based on a competitive training between two separate neural networks. In particular, GANs take advantage of the whole deep-learning machinery. A first neural-network is built called the generator. The generator's goal is to generate data similar to the ones of the dataset. They take as input a random number \mathbf{x} from a simple distribution $p(\mathbf{x})$ (from which it is easy to sample). The input is then transformed by a family of functions g_{θ} which is usually given by a neural network even though it is not mandatory. The generator, hence maps the input space toward the output space $\{\mathbf{y}\}$ following a set of non-linear transformations. We can define the probability distribution of the generator as follows

$$p_G(\mathbf{y}) = \int d\mathbf{x} p(\mathbf{x}) \delta(\mathbf{y} - g_{\theta}(\mathbf{x})) \quad (11)$$

In the general case, this probability distribution is intractable and thus cannot be maximized using ML methods. The training procedure for such a model is therefore particular. To train the generator to transform the random variables of the prior distribution to data similar to those of the dataset, we use an adversarial approach. A second neural network is built named Discriminator. The discriminator task will be to distinguish between dataset samples and generated data by the Generator. To do so, it takes as input either a sample from the dataset or a generated one, and, as output gives a probability of belonging to the true dataset. In general, a different neural network is used for the discriminator d_{λ} . Now, the training procedure works in the following two-steps procedure. In a first step, the Generator will adjust its weights such that it is able to fool the Discriminator. In a second step, the Discriminator will adjust its weights to distinguish better between the true and the generated samples. The following loss is used for the training of the generator:

$$\mathcal{L}_G = \int d\mathbf{y} d\mathbf{x} p(\mathbf{x}) \delta(\mathbf{y} - g_{\theta}(\mathbf{x})) \log [1 - d_{\lambda}(g_{\theta}(\mathbf{x}))] = \int d\mathbf{y} p_G(\mathbf{y}) \log [1 - d_{\lambda}(\mathbf{y})]$$

After one of many steps of minimizing the loss of the generator (there are many recipes which we will not enter into too much detail) the loss of the discriminator is then minimized. The discriminator task is to get better and better at distinguishing the true samples from the generated ones. To this purpose, It needs to minimize the following loss

$$\mathcal{L}_D = - \int p_{\text{dataset}}(\mathbf{y}) \log [d_{\lambda}(\mathbf{y})] - \int d\mathbf{y} p_G(\mathbf{y}) \log [1 - d_{\lambda}(\mathbf{y})]$$

In this second step, only the weights of the discriminator are adjusted while the generator is fixed. We also see that by the alternance of losses and by changing in each case only the weights of one of the two neural networks, we can use the loss of the discriminator and change the sign when optimizing for the generator.

The whole optimization scheme is quite unstable and, in fact, it is in general not easy to design a working GAN for your specific dataset. Therefore, if possible, it is wise to first find a working GAN in the literature and start to adjust the architecture from it.

This ends the Machine Learning introduction, with the definition of some well-known models. We switch now to the statistical physics part, where we will tackle these problems from a different perspective.

6. Perceptron: Computing the capacity

We will show in this section how to compute the capacity in the perceptron under some hypothesis over the dataset and, following statistical physics argument — or equivalently analyzing the typical behavior of the machine — rather than by looking at the convergence properties of the learning dynamics. In this context, the model was first analyzed by Gardner in the 80's [2, 26]. We make the same kind of computation following the development of [27]. But first, let's summarize what are the important questions on which we will focus on and the formalism that we will use to answer them:

- Can we compute the generalization error for a perceptron trained with a given number of training samples
- Can we compute the capacity: the number of patterns that can be retrieved/learned

To assess these questions, we shall do a “typical case” analysis. That is, at the contrary of the worst case analysis, that intends to understand the properties of the most difficult case, we will analyze the typical case, the one that we would face typically assuming some statistical ensemble. The analysis is quite different from the ML approach. We will not at all focus on the learning dynamics, which is still of course an important question. But we will rather look at a Teacher-Student (TS) scenario where, we will define an à priori distribution for the considered dataset and model and, try to look at the typical realization of them and analyse their properties.

6.1. Teacher-Student analysis

In the TS scenario, we first define a *teacher* perceptron, chosen from a distribution of possible teachers. The teacher will be an oracle providing us with the correct answer when classifying the training set. We will call the parameters of the teacher \mathbf{w}_T , and note the classification it provides as $y_T(\mathbf{x}) = \text{sgn}(\mathbf{x} \cdot \mathbf{w}_T)$. The main objective here will be to analyze the statistical properties of the *student*, another perceptron which intends to classify correctly the training dataset. The parameters of the student will be \mathbf{w}_S for its weights, its output is given by $y_S(\mathbf{x}) = \text{sgn}(\mathbf{x} \cdot \mathbf{w}_S)$

Let's add the following notation, the number of inputs will be denoted N_v . And the chosen training set will follow the distribution

$$p(\mathbf{x}) = \prod_i \left[\frac{1}{2} \delta_{x_i, -1} + \frac{1}{2} \delta_{x_i, 1} \right]$$

In general we will consider a training set of P samples:

$$\{\mathbf{x}^{(m)}, \tilde{y}^{(m)}\}_{m=1, \dots, P} \quad \text{where} \quad \tilde{y}^{(m)} = \text{sgn}(\mathbf{x}^{(m)} \cdot \mathbf{w}_T)$$

We can now define the error on the training set and the generalization error to be

$$\begin{aligned} \epsilon_t(\mathbf{w}_S, \{\mathbf{x}^{(m)}\}, \mathbf{w}_T) &= \frac{1}{P} \sum_m \theta(-y_T(\mathbf{x}^{(m)}) y_S(\mathbf{x}^{(m)})) \\ \epsilon_G(\mathbf{w}_S, \mathbf{w}_T) &= \sum_{\{\mathbf{x}\}} p(\mathbf{x}) \theta(-y_T(\mathbf{x}) y_S(\mathbf{x})) \end{aligned}$$

where $\Theta(x)$ is the Heaviside function. We see that the training error correspond to the ratio of misclassified samples evaluated from the training set, while the generalization error is computed with respect to the true distribution of the data.

Our typical case analysis will rely on what is called “Gibbs learning”. That is: instead of learning the weights of the perceptron using a stochastic gradient descent, we look at the space defined by all the possible students that classify correctly the training dataset and take one uniformly at random. Then, we will compute the generalization error of these “typical students”. To simplify the computation, we will consider that the parameters of the perceptron have a spherical constraint: $\|\mathbf{w}\|_2^2 = N_v$: they will live on the hyper-sphere in N_v -dimensions. This is only a minor constraint since the classification does not depend on the norm of the weights. With this construction, all datapoints which projection form an angle of less than $\pi/2$ with the teacher are classified +1, and the others −1. Therefore, if the student has an angle θ with the teacher, we can represent geometrically the volume of misclassified data as on fig. 7 left panel. Now, the generalization error given the angle θ is given by the ratio of all possible datapoints over the ones ending in the misclassified regions. The generalization error is thus given by $\epsilon_G = \frac{\theta}{\pi}$ where θ is the angle between \mathbf{w}_T and \mathbf{w}_S . We can thus express the generalization error in terms of the scalar product of the two perceptrons, writing $R = \mathbf{w}_T \cdot \mathbf{w}_S / N_v$ it gives $\epsilon_G = \arccos(R) / \pi$.

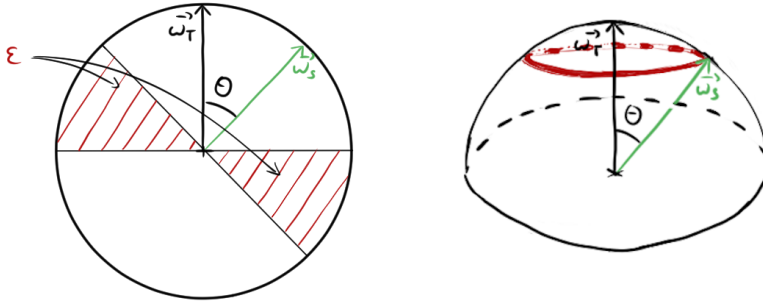


Figure 7: Left: graphical representation of the generalization error given a student vector w_S and a teacher w_T . Right: visualization of the volume of possible perceptrons with a given a generalization error in red.

The generalization error — We wish to answer the question: by taking uniformly at random a student perceptron classifying correctly the training set (amongst all the possible ones), what is the value of the generalization error ? To do that, we need to compute the volume of all perceptrons that classify correctly the training set. For that, we will make a large deviation computation. To begin, we can compute what is the volume of all student perceptrons sharing an overlap R with the teacher (hence fixing the generalization error), as illustrated on fig. 7 right panel. Doing this, we found

$$\Omega_0(\epsilon) = \int dw_S \delta(w_S^2 - N_v) \delta(R - \cos(\pi\epsilon)) \sim \exp\left(\frac{N_v}{2} [1 + \log(2\pi) + \log(\sin^2(\pi\epsilon))]\right) \quad (12)$$

where the details can be found in appendix 10.1. We see that this entropy will be exponentially dominated by the saddle point at $\epsilon^* = 1/2$. It means that, the number of perceptrons giving a classification error of $1/2$ is so huge, comparing to those having a smaller error, that it is impossible to find by chance a perceptron doing better than that. Therefore, taking a student uniformly at random will inevitably gives a result equivalent to randomly guessing the sign of y .

Now we can try to see what would be the effect of adding training samples. We add the constraint that the student parameters should classify correctly a number P of samples drawn randomly from the sample's a priori distribution. In our case, we will consider that the samples are uniformly distributed. The quantity we want can be expressed as

$$\Omega(w_T, \{x\}^{(m)}) = \int \frac{dw_S \delta(w_S^2 - N)}{(\int dw_S' \delta(w_S'^2 - N))} \prod_m \theta\left[\left(\frac{1}{\sqrt{N}} w_T \cdot x^{(m)}\right) \left(\frac{1}{\sqrt{N}} w_S \cdot x^{(m)}\right)\right]$$

where the denominator is here to normalize the whole expression. This expression depends on a particular realization of the training set and of the teacher parameters. In order to obtain the true quenched entropy, we need to compute

$$S = \langle \log(\Omega(w_T, \{x\}^{(m)})) \rangle_{w_T, x \sim p(x)}$$

Following [27], where the average is performed over the training set and all possible teachers. This term is in general harder to deal with. A first simpler approximation can be computed by considering the annealed case

$$S_P^{\text{ann}} = \log\left(\langle \Omega(w_T, \{x\}^{(m)}) \rangle_{w_T, x \sim p(x)}\right) = \log(\Omega_P)$$

where P indicates the number of considered training samples. The annealed case can be seen as an approximation of the true quenched computation. It is also true that in some cases, when the typical values of $\Omega(w_T, \{x\}^{(m)})$ are very peaked, the annealed computation gives the correct results. However, this usually happens in the high temperature regime (our analysis here is made at zero temperature), and it is not the case in our situation as we will see later. Still, the detail of the computation can be found in the appendix 10.2 and we give the main steps here for the annealed computation:

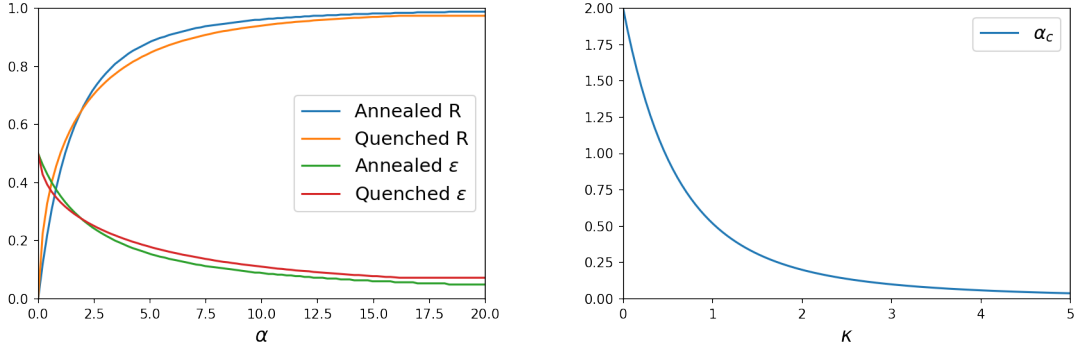


Figure 8: Left: The overlap R and the error obtained in the perceptron obtained as a function of $\alpha = P/N_v$. Right: The critical capacity of the perceptron as a function of the margin κ

1. Introducing Lagrange multipliers $\lambda_m = \frac{1}{\sqrt{N_v}} \mathbf{w}_S \cdot \mathbf{x}^{(m)}$ and $\tau_m = \frac{1}{\sqrt{N_v}} \mathbf{w}_T \cdot \mathbf{x}^{(m)}$ such that it is possible later to average over the dataset outside of the theta functions.
2. Using a Fourier representation of the delta function
3. At that point, it is possible to average over \mathbf{x}
4. Approximate the result at leading order in N_v within the exponential

The following expression is obtained

$$\Omega_P = \int_{-1}^1 dR \exp \left(N_v \left[1/2 \log(1 - R^2) + \alpha \log \left(1 - \frac{\arccos R}{\pi} \right) \right] \right)$$

where $\alpha = P/N_v$. Again, it is possible to compute the saddle point with respect to R for various values of α . We recover that when $\alpha = 0$, the entropy is dominated by $\epsilon_G = 1/2$. Then, as α increases, the value of ϵ_G decreases until it reaches zero as α goes to infinity.

To compute the quenched average, one has to use the replica trick. The replica trick uses the following identity

$$\log(x) = \lim_{n \rightarrow 0} \frac{x^n - 1}{n}$$

The trick is thus to use this in the average of the log of the entropy, and to consider that n is an integer. Then, we have n replicas of our perceptrons and therefore $\mathbf{w}_S^a, \mathbf{w}_T^a$ where $a = 1, \dots, n$. After performing the average over the disorder, the following order parameter is introduced

$$q^{ab} = \frac{\mathbf{w}_S^a \cdot \mathbf{w}_S^b}{N_v}$$

$$R^a = \frac{\mathbf{w}_T^a \cdot \mathbf{w}_S^a}{N_v}$$

namely the overlap between the replicated students, and the overlap between the students and the teacher. To finish the computation, an ansatz should be taken for q and R . The most simple one is the *replica symmetry* ansatz where all replicas are identical. Most of the details of the computation is given in appendix 10.2. The overall result is given by

$$S \sim N_v \max_R \left[\frac{1}{2} \log(1 - R) \frac{R}{2} + \alpha \int \frac{dx}{\sqrt{2\pi}} e^{-x^2/2} \text{erfc} \left(-\sqrt{\frac{2R}{1-R}} x \right) \log \left(\text{erfc} \left(-\sqrt{\frac{2R}{1-R}} x \right) / 2 \right) \right]$$

where erfc is the complementary error function. On fig. 8 we show the result of both the annealed and the quenched computations. We see that in both cases we obtain the correct result when $\alpha = 0$, while the annealed approximation is slightly underestimating the error for increasing value of α . To show the correctness of the replica symmetric ansatz, it is needed to check the stability of the solution with respect to the so-called replica symmetry breaking solutions. This falls out of the scope of this lecture but it is important to know that in many systems, more elaborated parametrization of the replica parameters q^{ab} and R^a must be found in order to obtain the correct result.

6.2. Capacity of the network

Another interesting question that arises is about the capacity of the network, or to rephrase, the number of patterns that can be learned by the perceptron. In this context, we do not need a teacher, but only a set of P training samples $\{\mathbf{x}^{(m)} \tilde{y}^{(m)}\}$ for $m = 1, \dots, P$ that will be used as patterns. We want now to impose that the perceptron is capable of classifying correctly these samples (or patterns), imposing the following condition on the student weights

$$\frac{1}{\sqrt{N_v}} \tilde{y}^{(m)} \mathbf{w}_S \cdot \mathbf{x}^{(m)} \geq \kappa \quad \forall m = 1, \dots, P \quad (13)$$

where we introduced κ , a positive constant ensuring a small margin of error. With this condition, we can again count the number of compatible solutions. In this case we do not have teacher and therefore we do not need to impose any overlap with an oracle. Therefore,

$$\Omega(\{\mathbf{x}^{(m)} \tilde{y}^{(m)}\}_m) = \int d\mathbf{w}_S \delta(\mathbf{w}_S^2 - N) \prod_m^P \theta\left(\frac{1}{\sqrt{N_v}} \tilde{y}^{(m)} \mathbf{w}_S \cdot \mathbf{x}^{(m)} - \kappa\right)$$

Using again the replica trick to compute the quenched entropy, it is possible for a given value of κ to compute the value α_c below which there exists an exponential number of perceptrons capable of learning the patterns, while for higher values of α , it is impossible. The result is given by the following condition

$$\frac{1}{\alpha_c} = \int_{-\infty}^{\kappa} \frac{dx}{\sqrt{2\pi}} e^{-x^2/2} (\kappa - t)^2$$

On fig 8, we show the behavior of the critical capacity, where we can observe how it decreases as the margin increases.

This concludes the main discussions on the Perceptron. We saw that approaches using statistical physics can lead to answer interesting questions on fundamental properties of the Perceptron. We will now depart from supervised learning to discuss results on a generative model.

7. From Perceptron to Hopfield to Restricted Boltzmann Machines

We can now make a series of connections, starting from the relation between the perceptron and the Hopfield model[28]. Then, we will see how the Hopfield model can be rephrased as a Restricted Boltzmann Machine. Instead of focusing on the patterns a Perceptron can learn, we can deal with another point of view. Can we define a “simple” dynamics over the samples/patterns \mathbf{x} , such that they are both the fixed points of the dynamics and attractors? To clarify this, we can imagine that instead of having one perceptron, we could define a set of N_v perceptrons, where \mathbf{w}_i are the weights of the perceptron i . Then using eq. 3 for all the perceptron and stacking them together, we can define the following dynamics between the output of the set of perceptrons and a new input

$$x_i(t+1) = \text{sgn}\left(\sum_j w_{ij} x_j(t)\right) \quad (14)$$

Here $x_i(t)$ is the output of the perceptron i at step t . Then, this output is re-injected as input for the next step of the dynamics. For each of them, we could impose that the patterns are fixed point of the dynamics, meaning that the output of the perceptron i reproduces the input i all the time. Hence, dropping the time indices in eq. 14 and writing that the product of the l.h.s. should be of the same sign as the argument of the sign function, we obtain the following set of conditions over all patterns/samples m :

$$x_i^{(m)} \sum_j w_{ij} x_j^{(m)} \geq \kappa \quad \forall m = 1, \dots, P \text{ and } \forall i = 1, \dots, N_v$$

where again κ can be introduced to have a greater stability under the dynamics of eq. 14. We see that it is directly related to the storage problem of the perceptron, as can be seen by comparing it to eq. 13. Now, let's observe that the dynamical process of eq. 14 matches the zero-temperature dynamics of an Ising model where the couplings are given by the weight matrix w_{ij} . Hence using the Hamiltonian

$$\mathcal{H} = - \sum_{i < j} w_{ij} x_i x_j$$

Then, the steady-state patterns can be imposed in the dynamics by the following rule:

$$w_{ij} = \frac{1}{N_v} \sum_m x_i^{(m)} x_j^{(m)}$$

This is named the Hebb rule. Plugging this weight matrix in the equations of the dynamics eq. 14, it is easy to verify that the patterns are fixed points of the dynamics. Let's consider that the input is in the pattern (n) at time t : $x_i(t) = x_i^{(n)}$, we can write

$$x_i(t+1) = \text{sgn} \left(\frac{1}{N_v} \sum_{j,m} x_i^{(m)} x_j^{(m)} x_i(t) \right) \approx \text{sgn} \left(\frac{1}{N_v} x_i^{(n)} \right) = x_i^{(n)}$$

where we used the fact that the patterns are orthogonal in the large N_v limit and the last equality stands if the variable $x_i(t)$ was in the pattern (n) . In fact, the corresponding Ising model has been studied for a long time and is known under the name of Hopfield model. In the Hopfield model, the patterns are typically drawn from the Bernoulli distribution: $\xi_i^\mu = \pm 1$ with probability one-half. We will now index our samples by μ (instead of m so to not confuse it with the magnetization), and name the variables s to refer to them as spins. This gives the following Boltzmann distribution

$$p[s] = \frac{1}{Z} \exp \left[\frac{\beta}{N_v} \sum_{\mu} \sum_{i < j} \xi_i^\mu \xi_j^\mu s_i s_j \right] = \frac{1}{Z} \exp \left[\frac{\beta}{2N_v} \sum_{\mu} \left(\sum_i \xi_i^\mu s_i \right)^2 \right]$$

In the zero temperature limit, we have seen that the patterns are stable with respect to the dynamics of eq. 14. Interestingly, the model also presents interesting equilibrium properties for a wide range of temperature depending on the number of patterns $P = \alpha N_v$. It is possible to understand quickly what happens in the low storage regime, when $P \ll N_v$, ($\alpha \sim 0$). In this regime, we can approximate the partition function as follows by using the Hubbard-Stratonovitch transformation to linearize the interaction term

$$\begin{aligned} Z &= \int d\mathbf{m} \exp \left(-N\beta \mathbf{m}^2/2 + \sum_i \log \left[\cosh \left(\beta \sum_{\mu} \xi_i^\mu m_{\mu} \right) \right] \right) \\ &\approx \exp \left(-N\beta \hat{\mathbf{m}}^2/2 + \sum_i \log \left[\cosh \left(\beta \sum_{\mu} \xi_i^\mu \hat{m}_{\mu} \right) \right] \right) \text{ where } \hat{m}_{\mu} = \frac{1}{N_v} \sum_i \xi_i^\mu \tanh \left[\beta \sum_{\mu} \xi_i^\mu m_{\mu} \right] \end{aligned} \quad (15)$$

The solutions to this equation can be found by choosing the projected magnetization $\hat{\mathbf{m}}$ to be one along a given pattern and zero along the others. This gives the following mean-field self-consistent equation:

$$m = \tanh(\beta m)$$

which implies a second order phase transition at $\beta_c = 1$, as one recalls from the Curie-Weiss model⁴. In this simple case, the Hopfield model behaves as a ferromagnet where the equilibrium low temperature phase corresponds to the retrieval of one pattern among all the possible ones.

When the number of pattern becomes proportional to the system size $P = \alpha N_v$, we have to take care of the possible correlation between the patterns. In that case indeed, the proper treatment is to introduce the replica trick to compute the quenched free energy. We pass the details of the computation that can be found in [7] and comment quickly the phase diagram that is reproduced on fig. 9. We now have many interesting regions. In particular, when α is below a given threshold, the equilibrium configurations of the system do correspond to the patterns: it is the retrieval stable region. Then, at a given temperature, by increasing α the system will enter into a regime where a mixture of patterns can become dominant, the retrieval metastable region. Finally, for large α and low-temperature spurious states appear in the spin glass phase, as a consequence of having too many patterns.

The phase diagram of the Hopfield model is interesting as it explains how orthogonal patterns can be stored and retrieved by modelling the equilibrium state of a Boltzmann distribution. However, the fact that the interactions between the spins is pairwise, limits the “expressivity” of this model. In particular, if we were to use the Hopfield model as

⁴Other solutions can be found, but they are not dominating in free energy

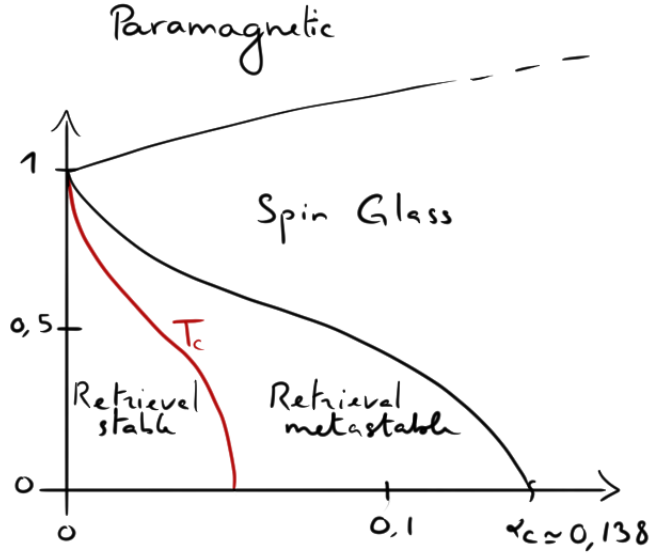


Figure 9: Phase diagram of the Hopfield model. For low values of α , the critical temperature is equal to one, as in the Curie-Weiss model. When it starts to be proportional to the number of spins, two interesting phases arise: the retrieval where the pattern are stable and the one where they are metastable.

a generative model for a complex dataset, it will be impossible to adjust the higher-moments of the data distribution. Still, by using the transformation we used to compute Z in eq. 15, we can write the probability distribution of the Hopfield using a Hamiltonian defined on a bipartite network,

$$p[s, m] = \frac{1}{Z} \exp \left(-N \beta m^2 / 2 + \beta \sum_{i, \mu} s_i \xi_i^\mu m_\mu \right) \quad (16)$$

being one layer composed by a set of discrete variables s_i , and another of the continuous Gaussian ones m_μ , that we introduced to linearize the Hopfield's Hamiltonian. Note in particular there are no interactions amongst the spins or the Gaussian fields.

Starting from the same topology (a bipartite network where only half is related to the patterns we want to retrieve), we can generalize it by adjusting the type of variables that we are considering, this is what defines the RBM. The prior distribution that we choose for the s_i will control the way we modelize our data, while the prior we choose over the variables m_μ will impact the effective Hamiltonian we obtain after integrating over them. In the classical RBMs, the variables m_μ are usually either discrete or truncated Gaussians. We illustrate here why taking discrete values is an improvement over the Hopfield model. Recall that if we choose the m_μ to be Gaussian, we will recover the Hopfield model. Now, if we choose the m_μ to be discrete, the effective Hamiltonian obtained after marginalizing these variables is

$$\begin{aligned} \mathcal{H}_{\text{eff}}[s] &= \sum_{\mu} \log \left[\cosh \left(\sum_i \xi_i^\mu s_i \right) \right] \approx \sum_{\mu} \log \left[1 + \frac{1}{2} \left(\sum_i \xi_i^\mu s_i \right)^2 + \frac{1}{4!} \left(\sum_i \xi_i^\mu s_i \right)^4 + \dots \right] \\ &\approx \frac{1}{2} \sum_{i,j} s_i \sum_{\mu} \xi_i^\mu \xi_j^\mu s_j - \frac{7}{4!} \sum_{\mu} \sum_{i,j,k,l} s_i s_j s_k s_l \xi_i^\mu \xi_j^\mu \xi_k^\mu \xi_l^\mu + \dots \end{aligned}$$

By expanding the log cosh in the above equation, we see that at the second order in ξ we recover the Hopfield model. But now, higher orders are present and the weights ξ_i^μ can be adjusted to fit best the considered dataset⁵. We will now focus on the thermodynamics properties and the learning equations of such a machine.

8. Restricted Boltzmann Machine: a generative model of spins

We understand now that RBM can be progressively derived from the Hopfield model. In this interpretation, the weights of the RBM can be interpreted as patterns that are learned. In the following, we will see into more detail the learning equations of the RBM, and derive its phase diagram in a simplified mean-field context. For the rest of the section, we will note the hidden variables τ (instead of the m_μ above) and keep the variables to be discrete.

8.1. Learning an RBM

We will derive the learning equations of the RBM for discrete $\{0, 1\}$ variables for both the visible and hidden layers. The generalization to other prior distributions is quite straightforward. Let's first introduce the following notations. The average over the RBM distribution will be noted as

$$\langle f(s, \tau) \rangle_{\mathcal{H}} = \sum_{\{s, \tau\}} p(s, \tau) f(s, \tau) \quad (17)$$

Before entering more into the technical details about the RBM, it is important to recall that it has been designed as a "learnable" generative model in practice. In that sense, the usual procedure is to feed the RBM with a dataset, tune its parameters \mathbf{w} , $\boldsymbol{\theta}$ and $\boldsymbol{\eta}$ such that the equilibrium properties of the learned RBM reproduce faithfully the correlations (or the patterns) present in the dataset. In other words, it is expected that the learned model is able to produce new data statistically similar but distinct from the training set. To do so, the classical procedure is to proceed with a stochastic gradient ascent of the likelihood function that can be easily expressed. Usually the learning of ML models involves the minimization of a loss function which happens here to be minus the log likelihood, which we will minimize by means of the classical Stochastic Gradient Descent (SGD) algorithm. First, consider a set of datapoints $\{s_i^{(d)}\}$, where $d = 1, \dots, M$ is the index of the data. The log-likelihood is given by

$$\begin{aligned} \mathcal{L} &= \frac{1}{M} \sum_{d=1}^M \log \left(\sum_{\{\tau\}} p(s^{(d)}, \tau) \right) = \frac{1}{M} \sum_{d=1}^M \log (p(s^{(d)})) \\ &= \frac{1}{M} \sum_{d=1}^M \left[\log \left(\sum_{\tau \in \{0,1\}} \exp(-\mathcal{H}[s^{(d)}, \tau]) \right) \right] - \log(Z) \\ &= \frac{1}{M} \sum_{d=1}^M \left[\sum_i \theta_i s_i^{(d)} + \sum_\mu \log \left(1 + \exp \left(\sum_i s_i^{(d)} w_{i\mu} + \eta_\mu \right) \right) \right] - \log(Z) \end{aligned}$$

Note here that in the usual definition of the RBM, external fields $\boldsymbol{\theta}$ and $\boldsymbol{\eta}$ are present. The gradient w.r.t. the different parameters will then take a simple form. Let us detail the computation of the gradient w.r.t. the weight matrix. By deriving the log-likelihood w.r.t. the weight matrix we get

$$\begin{aligned} \frac{\partial \mathcal{L}}{\partial w_{i\mu}} &= \frac{1}{M} \sum_{d=1}^M \frac{s_i^{(d)}}{1 + \exp(\sum_i s_i^{(d)} w_{i\mu} + \eta_\mu)} - \langle s_i \tau_\mu \rangle_{\mathcal{H}} \\ &= \frac{1}{M} \sum_{d=1}^M s_i^{(d)} p(\tau_\mu = 1 | s^{(d)}) - \langle s_i \tau_\mu \rangle_{\mathcal{H}} \\ &= \langle s_i \tau_\mu \rangle_{\text{data}} - \langle s_i \tau_\mu \rangle_{\mathcal{H}} \end{aligned} \quad (18)$$

where we used the following notation

$$\langle f(s, \tau) \rangle_{\text{data}} = \frac{1}{M} \sum_{d=1}^M f(s^{(d)}, \tau) p(\tau | s^{(d)}), \quad (19)$$

⁵Note that we do not have explicit odd-order in the expansion because of the lack of external fields in the original Hamiltonian. Odd terms would appear in a more general case

that is the average over the dataset samples. The gradients for the biases (or magnetic fields) can be obtained similarly

$$\frac{\partial \mathcal{L}}{\partial \theta_i} = \langle s_i \rangle_{\text{data}} - \langle s_i \rangle_{\mathcal{H}} \quad (20)$$

$$\frac{\partial \mathcal{L}}{\partial \eta_\mu} = \langle \tau_\mu \rangle_{\text{data}} - \langle \eta_\mu \rangle_{\mathcal{H}} \quad (21)$$

It is interesting to note that, in expression (18), the gradient is very similar to the one obtained in the traditional inverse Ising problem with the difference that in the inverse Ising problem the first term on the r.h.s. (sometimes coined “positive term”) depends only on the data, while for the RBM, we have a dependence on the model through the hidden variables (yet simple to compute), see the appendix 10.4 for a quick presentation of the Ising inverse case. Once the gradient is computed, the parameters of the model are updated following the rules

$$w_{i\mu}^{(t+1)} = w_{i\mu}^{(t)} + \gamma \frac{\partial \mathcal{L}}{\partial w_{i\mu}} \Big|_{w_{i\mu}^{(t)}, \theta_i^{(t)}, \eta_\mu^{(t)}} \quad (22)$$

$$\theta_i^{(t+1)} = \theta_i^{(t)} + \gamma \frac{\partial \mathcal{L}}{\partial \theta_i} \Big|_{w_{i\mu}^{(t)}, \theta_i^{(t)}, \eta_\mu^{(t)}} \quad (23)$$

$$\eta_\mu^{(t+1)} = \eta_\mu^{(t)} + \gamma \frac{\partial \mathcal{L}}{\partial \eta_\mu} \Big|_{w_{i\mu}^{(t)}, \theta_i^{(t)}, \eta_\mu^{(t)}} \quad (24)$$

where γ , called the learning rate, tunes the speed at which the parameters are updated in a given direction, the superscript t being the index of iteration.

The difficulty to train an RBM lies in the computation of the second term of the gradient, the so-called “negative term”, which represents the correlation between a visible node i , and a hidden node a , under the RBM distribution. Depending on the value of the parameters of the model (the couplings and the biases), we can either be

1. in a phase where it is easy to sample configurations from $p(\mathbf{s}, \boldsymbol{\tau})$, — usually called paramagnetic phase —
2. in a spin glass phase (if unlucky), where it is exponentially hard to escape from the spurious free energy minima;
3. in a “recall” phase where the dominant states correspond to data-like configurations.

But even in the latter case, it might be difficult to compute the negative term when the free energy of the model presents many “good” minima. In fact, to transit from one state to another one with local stochastic move, the time is exponential in the size of the free energy barrier which is extensive in the system’s size. This makes the task of sampling the model very difficult, in particular it is a phenomenon present also in simpler models, such as for instance the Hopfield model.

8.2. Sampling and Approximation of the negative term

Before finishing with the learning algorithm of the RBM, we need to approach into a bit more detail how the sampling of this machine is done. In practice, any Markov Chains Monte Carlo could be used to sample the equilibrium configurations of the RBM. This task is not only important to generate samples from properly trained RBM, but it is also necessary to evaluate the “negative term” of the gradient. Interestingly, the architecture of the RBMs gives us a very simple heat-bath algorithm to perform MC iteration. First, let’s remark that the conditional probability of the visible nodes, when fixing the hidden ones (or vice-versa), factorises as

$$p(\mathbf{s}|\boldsymbol{\tau}) = \prod_i \frac{1}{1 + \exp(\sum_a w_{i\mu} \tau_\mu + \theta_i)} \text{ and therefore } p(s_i|\boldsymbol{\tau}) = \text{sig}(\sum_\mu w_{i\mu} \tau_\mu + \theta_i) \quad (25)$$

$$p(\boldsymbol{\tau}|\mathbf{s}) = \prod_\mu \frac{1}{1 + \exp(\sum_i w_{i\mu} s_i + \eta_\mu)} \text{ and therefore } p(\tau_\mu|\mathbf{s}) = \text{sig}(\sum_i w_{i\mu} s_i + \eta_\mu) \quad (26)$$

This property allows us to design a block-sampling algorithm that is commonly used for RBMs. First, you define the initial condition for the visible nodes \mathbf{s} (for instance, uniformly at random). Then, using eq. 26 we can sample directly all hidden nodes independently of each other using their Bernoulli distribution. Then, the same can be done to sample back the visible nodes, fixing the value of the hidden variables and sampling new states for the visible ones using eq. 25. Since this procedure respects the detailed balance, we are (in theory) sure that we would reach equilibrium configurations by running this MC algorithm long enough.

The negative term of the gradient can therefore be computed using various MCMC chains in parallel, updating each of them with the block sampling method, which is very efficient since most of the operation can be parallelized. In practice, there have been designed different schemes to reduce the number of MC steps needed. We list below the most classical ones with their eventual drawback.

- **Contrastive Divergence (CD)-k**: this method introduced by Hinton[29], consists in initializing the MC chains on the data of the minibatch to compute the gradient, and then to perform k MC steps (with k of order 1 usually). If this method does manage to learn some relevant features, we should warn that the learned RBM cannot be used at all for sampling when k is too small (which is the usual setup) and therefore to generate new decorrelated data. In fact, when the machine starts to learn, the number of steps is too small to depart from its initial condition and therefore the chains are very biased towards it.
- **Persistent CD (PCD)-k**: this is an improvement over CD. The first MC chains are started from random initial condition. Then, the final states of the chains are reused as the initial conditions for the next computation of the gradient. So, in practice, we are keeping always the same chain (there is not reset), and at each computation of the gradient, k steps are performed. For this learning dynamics, it has been observed that the learned RBM can reach almost equilibrium, in the sense that sampling new data from the learned machine will indeed be very similar to the data of the dataset. However, the quality of the generated samples will depend on the value of k , the larger the better, obviously.
- **Random (Rdm)-k**: this is the most naïve way to compute the negative term, where the MC chains are started from random initial conditions at each update of the gradient, and then k steps are performed. If this method is doomed to fail as soon as k gets lower than the MC mixing time – the time it takes to converge to equilibrium, — it has some very interesting biases. In fact, when the mixing time of the system increases (which arrives eventually during the learning), the chains can not reach equilibrium configurations[30]. At that point, an interesting phenomenon occurs, which is that the RBM learns to match the correlation of the dataset (and response of the hidden nodes) when repeating the exact same dynamics. In brief, when keeping the exact same dynamics (fixed k and the distribution used for the initial conditions), the RBM will learn a dynamical process: starting from the same precise initial conditions and performing the same number k of MC steps, the samples converge towards good samples. Sampling for larger times will end up in eventually reaching the equilibrium configurations of the learned model, which usually poorly represent the dataset. Of course, it is also possible to use this dynamics taking k very large such that the training is equilibrated during the whole training. In that case, the model is correctly trained but it is in general very costly.

Before concluding, we should also mention an approach more familiar in Physics. The negative term can also be approximated by a mean-field estimation of the correlations. A simple mean-field approach here would be to use a high-temperature — or small weights — approach[31, 32]. In this expansion, the mean-field magnetization of the visible and hidden nodes are given by the solutions of the self-consistent equations

$$m_i^{(v)} = \text{sig} \left(\sum_a w_{i\mu} m_\mu^{(h)} + \theta_i \right) \quad (27)$$

$$m_\mu^{(h)} = \text{sig} \left(\sum_i w_{i\mu} m_i^{(v)} + \eta_\mu \right) \quad (28)$$

Therefore, using the mean-field approximation the free energy to compute the derivative of $\log(Z)$, we end up with

$$\langle s_i \tau_\mu \rangle_{\mathcal{H}} \approx m_i^{(v)} m_\mu^{(h)} \quad (29)$$

where the mean-field values of the magnetization are obtained by solving iteratively the eqs. 27-28. This approximation can also be integrated in the different approach developed for Monte Carlo methods: CD-MF, PCD-MF or Rdm-MF. In practice, the same limitations discussed above apply for the mean-field case. With the learning rules discussed in this section, we shall be able to learn any dataset that is binary-discrete using the algorithm 2.

This is all about the basic practical aspects of the learning part. More works on the dynamical aspects can be found here[33, 30, 14], where both theoretical and numerical behaviors are inspected. However, so far, the long term behavior of the dynamics for complex dataset is not well understood.

Algorithm 2 RBM learning

Input: Data: $\mathbf{X} \in \mathbb{R}^{N \times D}$, hyper-parameters: $\Theta = N_h, \gamma, \text{MB}$, initialization: $\mathbf{w}^{(t=0)} \sim \mathcal{N}(0, \sigma)$, $\boldsymbol{\eta}^{(t=0)} = \mathbf{0}$, $\boldsymbol{\theta}^{(t=0)} = \mathbf{0}$.
Output: $\mathbf{w}^{(T)}$, $\boldsymbol{\eta}^{(T)}$, $\boldsymbol{\theta}^{(T)}$.
while $t \leq T$ **do**
 Compute l.h.s term of the gradient, eq. 18-21 using the RBM at t
 Compute the r.h.s. of eq. 18-21 using your preferred Monte Carlo approximation iterated for k steps
 Update the weights and biases using eq. 22-24
 $t \leftarrow t + 1$
end while

8.3. Phase Diagram of RBM

Deriving the phase diagram of RBM is not a simple question. Amongst the many reasons, a strong one is that we need to decide under what distribution of the weight matrix we want to do the computation. A classical approach when dealing with disordered systems is to consider that the quenched variables, here the weights (or patterns in the Hopfield model), are i.i.d. from the same distribution, e.g. Gaussian variables or discrete ± 1 . Similar approach has been studied for RBMs [13, 34] allowing the computation of the phase diagram. Yet, we can argue that during the learning, it is rather unlikely that the weights remain independent after many epochs. In this lecture's note we will rather adapt the formalism from [14], which departs a bit from the classical approach. Instead of considering independent weights, we will rather use the following assumption of a low rank- K matrix decomposition for the weight matrix \mathbf{w} — as if doing a singular value decomposition (SVD) and keeping the first K modes —

$$w_{i\mu} \approx \sum_{\alpha=1}^K u_i^\alpha w_\alpha v_\mu^\alpha$$

The idea is to consider that the eigenvalues w_α are encoding the structure of the dataset while we will be averaging over the rotation matrices \mathbf{u} and \mathbf{v} . Using this decomposition, we can rewrite the replicated partition function

$$\begin{aligned} Z^n &= \sum_{s, \tau} \exp \left[\sum_{a=1}^n \sum_{i, \mu, \alpha} s_i^a u_i^\alpha w_\alpha v_\mu^\alpha \tau_\mu^a + \dots \right] = \sum_{s, \tau} \exp \left[\sum_{a, \alpha} w_\alpha \left(\sum_i s_i^a u_i^\alpha \right) \left(\sum_\mu v_\mu^\alpha \tau_\mu^a \right) + \dots \right] \\ &= \int \prod_{\alpha, a} \frac{d m_\alpha^a d \bar{m}_\alpha^a}{2\pi} \sum_{s, \tau} \prod_a \exp \left[-L \sum_\alpha \left(w_\alpha (m_\alpha^a \bar{m}_\alpha^a - m_\alpha^a s_\alpha^a - \bar{m}_\alpha^a \tau_\alpha^a) + \eta_\alpha s_\alpha^a + \theta_\alpha \tau_\alpha^a \right) \right] \end{aligned} \quad (30)$$

where we introduced the following quantities

$$\begin{aligned} L &= \sqrt{N_v N_h}, \quad \text{and later we will also use } \kappa = \frac{N_h}{N_v} \\ s_\alpha^a &= \frac{1}{\sqrt{L}} \sum_i s_i^a u_i^\alpha \quad \text{and} \quad \eta_\alpha = \frac{1}{\sqrt{L}} \sum_i \eta_i u_i^\alpha \\ \tau_\alpha^a &= \frac{1}{\sqrt{L}} \sum_\mu \tau_\mu^a v_\mu^\alpha \quad \text{and} \quad \theta_\alpha = \frac{1}{\sqrt{L}} \sum_\mu \theta_\mu v_\mu^\alpha \end{aligned}$$

We project our spin variables over the SVD decomposition of the weight matrix. Using the hypothesis that the rotation matrix \mathbf{u} and \mathbf{v} are made of i.i.d. elements and taking the terms linear in n , the number of replicas, we get the following expression for the free energy (see appendix 10.5 for details) and the following order parameters

$$\begin{aligned} f[m, \bar{m}] &= \sum_\alpha w_\alpha m_\alpha \bar{m}_\alpha - \frac{1}{\sqrt{\kappa}} \mathbb{E}_u [\log 2 \cosh(h(u))] - \sqrt{\kappa} \mathbb{E}_v [\log 2 \cosh(\bar{h}(v))] \\ m_\alpha &= \kappa^{\frac{1}{4}} \mathbb{E}_v [v^\alpha \tanh(\bar{h}(v))] \quad \text{and} \quad \bar{m}_\alpha = \kappa^{-\frac{1}{4}} \mathbb{E}_u [u^\alpha \tanh(h(u))] \end{aligned}$$

where we defined

$$h(u) = \kappa^{\frac{1}{4}} \left(\sum_{\gamma} (w_{\gamma} m_{\gamma} - \eta_{\gamma}) u^{\gamma} \right) \quad \text{and} \quad \bar{h}(v) = \kappa^{-\frac{1}{4}} \left(\sum_{\gamma} (w_{\gamma} m_{\gamma} - \theta_{\gamma}) v^{\gamma} \right)$$

Now, assuming a Gaussian distribution for the \mathbf{u} and \mathbf{v} , we can even simplify more the expression of the order parameters, obtaining the following

$$\begin{aligned} m_{\alpha} &= (w_{\alpha} \bar{m}_{\alpha} - \theta_{\alpha})(1 - q) \\ \bar{m}_{\alpha} &= (w_{\alpha} m_{\alpha} - \eta_{\alpha})(1 - \bar{q}) \\ q &= \mathbb{E}_v [\tanh^2(\bar{h}(v))] \\ \bar{q} &= \mathbb{E}_u [\tanh^2(h(u))] \end{aligned}$$

The interpretation of these order parameters is clear. The magnetization m_{α} and \bar{m}_{α} represent the macroscopic magnetization of the system projected along the K modes of the weight matrix. The parameters q and \bar{q} represent the overlap (or spin-glass order parameter) of the visible and hidden nodes respectively. From these equations, we can identify a trivial solution corresponding to the existence of a paramagnetic phase, where $m_{\alpha} = \bar{m}_{\alpha} = q = \bar{q} = 0$. An interesting question is whether this phase is stable or not in general, or if there exists a ferromagnetic phase where the magnetization are not zero. We can compute the Hessian of the free energy to check the stability of the solution with respect to the ferromagnetic order parameter, and projected within the ferromagnetic phase. In such case, we obtain the following equations for the determinant of the Hessian

$$(1 - q)(1 - \bar{q})w_{\alpha}^2 = 1$$

Now, starting from the paramagnetic phase we fix $q = \bar{q} = 0$. We obtain that the paramagnetic phase is stable up to $w_{\alpha} = 1$ which determines the equivalent critical temperature of the model. Hence, under the hypothesis of low rank matrix \mathbf{w} and the independence of the elements of the rotations matrices \mathbf{u} and \mathbf{v} , we showed that a transition from a paramagnetic regime to a ferromagnetic one exists. The different phases can be studied with more details, but this falls out of scope of this lecture. However, an important result is that the macroscopic behavior of the ferromagnetic phase depends on the distribution taken for the rotation matrices. In fact, when taking Gaussian distribution, it is possible to show that only the condensation toward the strongest mode — the one with the highest w_{α} is stable. While, it is possible to obtain a mixture of modes by considering distributions with higher kurtosis. Again, in general it is important to check the stability of the replica symmetric ansatz as already discussed for the case of the Perceptron.

This concludes the last part on RBM. An important message here is that, physicists have brought interesting new directions to understand the static behavior as a function of its parameters. Yet, despite many works on this machine, most of its learning mechanisms remain scarcely understood when dealing with complex (hence real) datasets, and therefore leave much space for future work.

9. Acknowledgement

I'm indebted to the following colleagues that accepted to read this manuscript and helped me to improve it: Beatriz Seoane, Javier Moreno Gordo, Isidoro González-Adalid Pemartin. A.D. was supported by the Comunidad de Madrid and the Complutense University of Madrid (Spain) through the Atracción de Talento program (Ref. 2019-T1/TIC-13298).

10. Appendix

10.1. Generalization error without training samples

In the computation of the generalization error before seeing training samples, we can compute the typical generalization error. The formula is given by the saddle point of the following entropy

$$\Omega_0(\epsilon) = \int d\mathbf{w}_S \delta(\mathbf{w}_S^2 - N_v) \delta\left(\frac{\mathbf{w}_S \cdot \mathbf{w}_T}{N_v} - R(\epsilon)\right)$$

where $R(\epsilon) = \cos(\pi\epsilon)$. To compute this integral, we can use the Fourier representation of the delta distribution. We will then perform a saddle point computation w.r.t. the conjugate parameter associate to the spherical constraint.

$$\begin{aligned}
 \Omega_0(\epsilon) &= \int d\mathbf{w}_S \frac{dz d\lambda}{(2\pi)^2} \exp \left[-z(\mathbf{w}_S^2 - N_v) - i\lambda \left(\frac{\mathbf{w}_S \cdot \mathbf{w}_T}{N_v} - R \right) \right] \\
 &= \int \frac{dz d\lambda}{(2\pi)^2} \exp \left[zN_v + i\lambda R \right] \prod_i \left[\int dw_{S,i} \exp \left(-zw_{S,i}^2 - i\lambda \frac{w_{S,i} w_{T,i}}{N_v} \right) \right] \\
 &= \int \frac{dz d\lambda}{(2\pi)^2} \exp \left[zN_v + \frac{N_v}{2} \log(\pi/z) \right] \exp \left[-\frac{\lambda^2}{4N_v z} + i\lambda R \right] \\
 &= \int \frac{dz}{(2\pi)^2} \sqrt{4N_v z \pi} \exp \left[\frac{N_v}{2} (\log(\pi) - \log(z) + 2z - 2R^2 z) \right] = \int dz g(z) \exp \left(\frac{N_v}{2} f(z) \right)
 \end{aligned}$$

where we used the fact that the teacher is a vector of the sphere $\mathbf{w}_T^2 = N_v$. We can now compute the saddle point of the argument in the exponential. We find that

$$\begin{aligned}
 z^* &= \frac{1}{2(1 - R^2)} \\
 f(z^*) &= \log(2\pi) + \log(1 - R^2) + 1
 \end{aligned}$$

which give the asymptotic behavior of the entropy.

10.2. Annealed and quenched Perceptron entropy

Annealed case — We give some details about the computation of the annealed perceptron's entropy. We wish to compute

$$S_P^{\text{ann}} = \log \left\langle \Omega \left(\mathbf{w}_T, \{\mathbf{x}\}_{\mathbf{w}_T, \mathbf{x}} \right) \right\rangle$$

The main difficulty is to compute $\langle \Omega \left(\mathbf{w}_T, \{\mathbf{x}\}_{\mathbf{w}_T, \mathbf{x}} \right) \rangle = \Omega_P$. The average number of states, is given by

$$\Omega_P = \int d\mathbf{w}_S \delta(\mathbf{w}_S^2 - N_v) \prod_m \left\langle \theta \left(\left[\frac{1}{\sqrt{N_v}} \mathbf{w}_S \cdot \mathbf{x}^{(m)} \right] \left[\frac{1}{\sqrt{N_v}} \mathbf{w}_T \cdot \mathbf{x}^{(m)} \right] \right) \right\rangle$$

We can use Lagrange multiplier λ_m and τ_m for the argument in the Heaviside function using delta function and then use the Fourier representation of the δ s

$$\begin{aligned}
 \Omega_P &= \int d\mathbf{w}_S \delta(\mathbf{w}_S^2 - N_v) \prod_m \left\{ \frac{d\lambda_m d\tau_m dk_m dl_m}{(2\pi)^2} \theta(\lambda_m \tau_m) \left\langle \exp \left(-ik_m \left[\lambda_m - \frac{1}{\sqrt{N_v}} \mathbf{w}_S \cdot \mathbf{x}^{(m)} \right] \right) \right. \right. \\
 &\quad \left. \left. \times \exp \left[-il_m \left(\tau_m - \frac{1}{\sqrt{N_v}} \mathbf{w}_T \cdot \mathbf{x}^{(m)} \right) \right] \right\rangle \right\}
 \end{aligned}$$

From this point, first we can factorize the average over the data $p(\mathbf{x})$. In our case, independant variables, uniformly distributed in $\{\pm 1\}$ we can rewrite the part in the bracket as

$$\begin{aligned}
 \langle \cdot \rangle &= \exp(-ik_m \lambda_m - il_m \tau_m) \prod_i \sum_{x_i^{(m)}} p(x_i^{(m)}) \exp \left(\frac{x_i^{(m)}}{\sqrt{N_v}} (k_m w_{S,i} + l_m w_{T,i}) \right) \\
 &= \exp \left[-ik_m \lambda_m - il_m \tau_m + \sum_i \log \cos \left(\frac{1}{\sqrt{N_v}} (k_m w_{S,i} + l_m w_{T,i}) \right) \right]
 \end{aligned} \tag{31}$$

Now, expanding the cos and then the log at the second order, and using the fact that $||\mathbf{w}_T||^2 = ||\mathbf{w}_S||^2 = 1$ we will be able to perform the integral over the variables k_m and l_m :

$$\begin{aligned} \int \frac{dk_m dl_m}{(2\pi)^2} \langle \cdot \rangle &= \int \frac{dk_m dl_m}{(2\pi)^2} \exp \left[-\frac{k_m^2}{2} - \frac{l_m^2}{2} - ik_m \lambda_m - il_m \tau_m - k_m l_m R \right] \\ &= \frac{1}{2\pi(1-R^2)} \exp \left(-\frac{\lambda_m^2 + \tau_m^2 - 2\lambda_m \tau_m R}{2(1-R^2)} \right) \end{aligned}$$

For the last steps, we will introduced another delta function to impose that the scalar product between the student and the teacher is equal to R , which will decouple the integral over \mathbf{w}_S from the lagrange multiplier.

$$\Omega_P = \int d\mathbf{w}_S \delta(\mathbf{w}_S^2 - N_v) \int_{-1}^1 dR \delta(\mathbf{w}_S \cdot \mathbf{w}_T - R) \prod_m \int \frac{d\lambda_m d\tau_m}{2\pi\sqrt{1-R^2}} \theta(\lambda_m \tau_m) \exp \left(-\frac{\lambda_m^2 + \tau_m^2 - 2\lambda_m \tau_m R}{2(1-R^2)} \right)$$

We focus on the integral over the lagrange multipliers. The Heaviside function impose that both parameters should be of the same sign. Now we can rewrite the whole term as

$$\frac{2}{1-R^2} \int_0^\infty \frac{d\lambda_m d\tau_m}{2\pi} \exp \left(-\frac{\lambda_m^2 + \tau_m^2 - 2\lambda_m \tau_m R}{2(1-R^2)} \right) = 1 - \frac{1}{\pi} \arccos R$$

Putting all together and using the expression of eq. 12 we obtain in the limit of large N_v

$$S_P^{\text{ann}} = N_v \max_R \left[\frac{1}{2} \ln(1-R^2) + \alpha \ln \left(1 - \frac{1}{\pi} \arccos R \right) \right]$$

where we used the fact that $P = \alpha N_v$.

Quenched case — This case is much more complicated, we will however sketch a few steps to give a flavor of the type of computation and refer the reader to [27] for a more detailed derivation. First of all, we shall use the replica trick to compute this term. The replica trick is based upon the following identity

$$\langle \ln \Omega \rangle = \lim_{n \rightarrow 0} \frac{\langle \Omega^n \rangle - 1}{n}$$

Therefore, our task is now to compute the disordered average of Ω^n and then to identify the linear terms in n . In order to compute the average of Ω^n we will assume that n is an integer:

$$\Omega^n = \int \prod_{a=1}^n d\mathbf{w}_S^a \delta((\mathbf{w}_S^a)^2 - N_v) \prod_m \prod_{a=1}^n \theta \left(\left[\frac{1}{\sqrt{N_v}} \mathbf{w}_S^a \cdot \mathbf{x}^{(m)} \right] \left[\frac{1}{\sqrt{N_v}} \mathbf{w}_T \cdot \mathbf{x}^{(m)} \right] \right)$$

We see that the same path can be taken as the annealed case, with the different that we have now many students indexed by a . We therefore get in place of eq. 31, the following

$$\langle \cdot \rangle = \exp \left[-i \sum_a k_m^a \lambda_m^a - il_m \tau_m + \sum_i \log \cos \left(\frac{1}{\sqrt{N_v}} \left(\sum_a k_m^a w_{S,i}^a + l_m w_{T,i}^a \right) \right) \right]$$

where we now have an additional dependence in the replica of the system. The expansion of the cosine at the second order will couple the replica, and the argument in the exponential becomes

$$\sum_i \log \cos \left(\frac{1}{\sqrt{N_v}} \left(\sum_a k_m^a w_{S,i}^a + l_m w_{T,i}^a \right) \right) \approx -\frac{l_m^2}{2} - \frac{1}{2} \sum_a (k_m^a)^2 - l_m \sum_a k_m^a R^a - \sum_{a < b} q^{ab} k_m^a k_m^b \quad (32)$$

where the variables R^a and q^{ab} are introduced by mean of a delta function, and defined as

$$R^a = \frac{1}{N_v} \mathbf{w}_S^a \cdot \mathbf{w}_T$$

$$q^{ab} = \frac{1}{N_v} \mathbf{w}_S^a \cdot \mathbf{w}_S^b$$

which are respectively the overlap of the student a with the teacher, and the overlap between the students. Now, we will assume that all the replicas are equivalent, and therefore $q^{ab} = R^a = R$. Rewriting eq. 32 using this approximation we get

$$-\frac{1}{2}(l_m \mathbf{k}_m)^T \mathbf{A}(l_m \mathbf{k}_m) - \mathbf{b}^T(l_m \mathbf{k}_m) \text{ where } A_{ab} = \delta_{ab}(1 - R) + R\mathbf{1}_{ab} \text{ and } \mathbf{b} = i(\tau_m \lambda_m)$$

where $\mathbf{1}$ is the matrix where all elements are equal to one, and the indices runs of $n + 1$ values, since we have to include the teacher. The eigenvectors of the matrix \mathbf{A} are $e_0 = 1 + nR$ and $e_1 = 1 - R$, with degeneracy 1 and n respectively. The matrix \mathbf{A} can easily be inverted

$$\mathbf{A}_{ab}^{-1} = \frac{1 + nR}{(1 - R)(1 + nR)} \delta_{ab} - \frac{R}{(1 - R)(1 + nR)} \mathbf{1}_{ab}$$

Using this, we can integrate over the variables l_m and \mathbf{k}_m , obtaining for a given m

$$\left\langle \prod_a \theta \left(\left[\frac{1}{\sqrt{N_v}} \mathbf{w}_S^a \cdot \mathbf{x}^{(m)} \right] \left[\frac{1}{\sqrt{N_v}} \mathbf{w}_T \cdot \mathbf{x}^{(m)} \right] \right) \right\rangle = \int \frac{d\tau_m}{\sqrt{2\pi(1 + nR)}} \prod_a \frac{d\lambda_m^a}{\sqrt{2\pi(1 - R)}} \prod_a \theta(\lambda_m^a \tau_m) \\ \times \exp \left[-\frac{1}{2(1 - R)(1 + nR)} \left((1 + (n - 1)R)\tau_m^2 + (1 + (n - 1)R) \sum_a (\lambda_m^a)^2 - 2R\tau_m \sum_a \lambda_m^a - R \sum_{a \neq b} \lambda_m^a \lambda_m^b \right) \right]$$

This expression can be further simplified. First the theta functions can be incorporated in the limits of the integral. Then, by renaming $\tau_m \rightarrow \lambda_m^{n+1}$ we can rewrite the integral as

$$\langle \cdot \rangle = 2 \sqrt{\frac{2\pi(1 - R)}{2\pi(1 + nR)}} \int_0^\infty \prod_{a=1}^{n+1} \frac{d\lambda_m^a}{2\pi(1 - R)} \exp \left[-\frac{1}{2(1 - R)(1 + nR)} \left((1 + nR) \sum_a (\lambda_m^a)^2 - R \left(\sum_a \lambda_m^a \right)^2 \right) \right] \\ = 2 \sqrt{\frac{2\pi(1 - R)}{2\pi(1 + nR)}} \int_0^\infty \prod_{a=1}^{n+1} \frac{d\lambda_m^a}{2\pi(1 - R)} \int \frac{dt}{\sqrt{2\pi}} e^{-t^2/2} \exp \left[t \sum_a \lambda_m^a \sqrt{\frac{R}{(1 - R)(1 + nR)}} \right] \\ \times \exp \left[-\frac{1}{2(1 - R)(1 + nR)} \left((1 + nR) \sum_a (\lambda_m^a)^2 \right) \right]$$

where we linearized the square using the Hubbard-Stratonovitch transformation. Now we can simplify this by changing the limits of the integrals over λ_m^a . Reinserting also the product over the training samples we get

$$\prod_m \left\langle \prod_a \theta \left(\left[\frac{1}{\sqrt{N_v}} \mathbf{w}_S^a \cdot \mathbf{x}^{(m)} \right] \left[\frac{1}{\sqrt{N_v}} \mathbf{w}_T \cdot \mathbf{x}^{(m)} \right] \right) \right\rangle = \left[2 \int \frac{1}{\sqrt{2\pi}} e^{-t^2/2} \left\{ \int_{-\sqrt{\frac{R}{1-R}}t}^\infty \frac{dx}{\sqrt{2\pi}} e^{-x^2/2} \right\}^{n+1} \right]^{\alpha N_v}$$

The entropic term can now be calculated. In addition to the delta function over the spherical constraint, we have also the constrain on the overlap between the various replica, and between the replica and the teacher. To simplify the expression, we renamed our teacher as a $n + 1$ replica of the system. Under the replica symmetric hypothesis, it simplifies the expression as follows

$$S = \int \prod_a d\mathbf{w}^a \delta((\mathbf{w}^a)^2 - N_v) \prod_{a < b} \delta(\mathbf{w}^a \cdot \mathbf{w}^b - N_v R) \\ = \int \prod_a d\mathbf{w}^a dz_a \prod_{a < b} dq_{ab} \exp \left[-\sum_a z_a ((\mathbf{w}^a)^2 - N_v) - \sum_{a < b} (\mathbf{w}^a \cdot \mathbf{w}^b - N_v R) \right] \\ = \int \prod_a d\mathbf{w}^a dz_a \prod_{a < b} dq_{ab} e^{\sum_a z_a N_v + \sum_{a < b} q_{ab} R N_v} \prod_i \left\{ \int d\mathbf{w} \exp \left[-\sum_a z_a (\mathbf{w}^a)^2 - \sum_{a < b} q_{ab} \mathbf{w}^a \cdot \mathbf{w}^b \right] \right\}$$

We can define the matrix

$$\mathbf{A}_{ab} = 2z_a\delta_{ab} + (\mathbf{1}_{ab} - \delta_{ab})q_{ab}$$

and compute formally the gaussian integral over the parameters \mathbf{w} , obtaining

$$S = \int \prod_a dz_a \prod_{a<b} dq_{ab} \exp \left[\frac{N_v}{2} \log(2\pi) - \frac{N_v}{2} \text{Tr} \text{Log} \mathbf{A} + \sum_a z_a N_v + \sum_{a<b} q_{ab} R N_v \right]$$

We can evaluate now the whole integral using the saddle point method over the variables z_a and q_{ab} . We get

$$\begin{aligned} \frac{\partial}{\partial z_a} &= -\frac{N_v}{2} \frac{\partial A_{aa}}{\partial z_a} A_{aa}^{-1} + N_v = -N_v A_{aa}^{-1} + N_v \\ \frac{\partial}{\partial q_{ab}} &= -\frac{N_v}{2} \frac{\partial A_{ab}}{\partial q_{ab}} A_{ba}^{-1} - \frac{N_v}{2} \frac{\partial A_{ba}}{\partial q_{ab}} A_{ab}^{-1} + R N_v = -N_v A_{ab}^{-1} + R N_v \end{aligned}$$

From this we can compute the inverse matrix \mathbf{A}^{-1} and its eigenvalues. The results is given by

$$S \sim \exp \left[\frac{N_v}{2} \left(n \log(1 - R) + \frac{1}{2} \log(1 + nR) \right) \right]$$

Putting everything together, we obtain

$$\langle \Omega^n \rangle = \int dR \exp \left\{ N_v \left[\frac{n}{2} \log(1 - R) + \frac{1}{2} \log(1 + nR) + \alpha \log \left(2 \int \frac{1}{\sqrt{2\pi}} e^{-t^2/2} \left\{ \int_{-\sqrt{\frac{R}{1-R}} t}^{\infty} \frac{dx}{\sqrt{2\pi}} e^{-x^2/2} \right\}^{n+1} \right) \right] \right\}$$

Now, isolating the term proportional to n , we obtain that

$$\frac{\langle \ln \Omega \rangle}{N_v} = \max_R \left[\frac{1}{2} \log(1 - R) + \frac{R}{2} + 2\alpha \int \frac{1}{\sqrt{2\pi}} e^{-t^2/2} \left\{ \int_{-\sqrt{\frac{R}{1-R}} t}^{\infty} \frac{dx}{\sqrt{2\pi}} e^{-x^2/2} \right\} \log \left\{ \int_{-\sqrt{\frac{R}{1-R}} t}^{\infty} \frac{dx}{\sqrt{2\pi}} e^{-x^2/2} \right\} \right]$$

10.3. Equivalence between the RBM and the Hopfield model

We show the equivalence between the RBM and the Hopfield model[35, 36] when having discrete binary variables for the visible nodes and gaussian ones for the hidden layer. Let's consider the Hopfield model

$$p[s] = \frac{1}{Z} \exp \left[\frac{\beta}{N} \sum_{\mu} \sum_{i<j} \xi_i^{\mu} \xi_j^{\mu} s_i s_j \right] = \frac{1}{Z} \exp \left[\frac{\beta}{2N} \sum_{\mu} \left(\sum_i \xi_i^{\mu} s_i \right)^2 + \text{cte} \right]$$

Using the Hubbard-Stratonovitch transformation, we can linearize the square and rewrite it as

$$p[s] = \frac{1}{Z} \int d\mathbf{m} \exp \left[-\frac{\sqrt{N}(\mathbf{m})^2}{2} + \sqrt{\beta} \sum_{i\mu} s_i \xi_i^{\mu} m_{\mu} \right]$$

Now, we can interpret the integrand as a new probability distribution over the variables s and \mathbf{m}

$$p[s, \mathbf{m}] = \frac{1}{Z} \exp \left[-\frac{(\mathbf{m})^2}{2} + \sqrt{\frac{\beta}{N}} \sum_{i\mu} s_i \xi_i^{\mu} m_{\mu} \right]$$

Hence, the Hamiltonian of the RBM is related to the one of Hopfield according to the following change

$$\sqrt{\frac{\beta}{N}} \xi_i^{\mu} \rightarrow w_{i\mu}$$

10.4. Inverse Ising problem

The inverse Ising problem consists in matching the coupling constants of an Ising model such that it fits best a given dataset. Let's consider a dataset $\{s_i^{(m)}\}$ where $m = 1 \dots, M$ of discrete ± 1 variables, and the following Ising model

$$p[s] = \frac{1}{Z} \exp \left[\sum_{i < j} J_{ij} s_i s_j + \sum_i h_i s_i \right]$$

We wish to adjust the variables \mathbf{J} and \mathbf{h} to the dataset, hence to maximize the following likelihood

$$\mathcal{L} = \frac{1}{M} \left(\sum_m \sum_{i < j} J_{ij} s_i^{(m)} s_j^{(m)} + \sum_i h_i s_i^{(m)} - \log Z \right)$$

To maximize it, we can follow the gradient

$$\begin{aligned} \frac{\partial \mathcal{L}}{\partial J_{ij}} &= \frac{1}{M} \sum_m s_i^{(m)} s_j^{(m)} - \langle s_i s_j \rangle_{\mathcal{H}} \\ \frac{\partial \mathcal{L}}{\partial h_i} &= \frac{1}{M} \sum_m s_i^{(m)} - \langle s_i \rangle_{\mathcal{H}} \end{aligned}$$

The first term of each gradient corresponds respectively to the pair-wise correlation and the average of the dataset. In particular, these terms are constant all along the learning at the opposite of the RBM where it involves the response function of the hidden nodes, involving therefore the parameters of the model. The model is more similar to the case of RBM, where the correlation and average is now computed using the distribution at a given stage of the learning. The same learning dynamics can be used

$$\begin{aligned} J_{ij}^{(t+1)} &= J_{ij}^{(t)} + \gamma \frac{\partial \mathcal{L}}{\partial J_{ij}} \Big|_{J_{ij}^{(t)}, h_i^{(t)}} \\ h_i^{(t+1)} &= h_i^{(t)} + \gamma \frac{\partial \mathcal{L}}{\partial h_i} \Big|_{J_{ij}^{(t)}, h_i^{(t)}} \end{aligned}$$

and the likelihood is convex in the parameters.

10.5. Free energy of the RBM

We derive the equations to obtain the mean-field free energy of the RBM. For simplicity we do not consider the biases since they are very simple to deal with. We start by considering eq. 30

$$Z^n = \int \prod_{\alpha, a} \frac{dm_{\alpha} d\bar{m}_{\alpha}}{2\pi} \prod_a \exp \left[-L \sum_{\alpha} w_{\alpha} (m_{\alpha}^a \bar{m}_{\alpha}^a - m_{\alpha}^a s_{\alpha}^a - \bar{m}_{\alpha}^a \tau_{\alpha}^a) \right]$$

We can isolate the terms involving only m_{α}^a on one side and \bar{m}_{α}^a on the other. We obtain

$$\phi_E = \sum_{s, \tau} \exp \left[L \sum_{\alpha, a} w_{\alpha} (m_{\alpha}^a s_{\alpha}^a + \bar{m}_{\alpha}^a \tau_{\alpha}^a) \right] = \prod_i \sum_{\{s_i^a\}} \exp \left[\sqrt{L} s_i^a \sum_{\alpha, a} w_{\alpha} m_{\alpha}^a u_i^a \right] \prod_{\mu} \sum_{\{\tau_{\mu}^a\}} \exp \left[\sqrt{L} \tau_{\mu}^a \sum_{\alpha, a} w_{\alpha} \bar{m}_{\alpha}^a v_{\mu}^a \right]$$

Now if we consider our hypothesis of i.i.d. variables for the quenched disorder \mathbf{u} and \mathbf{v} , we obtain

$$\begin{aligned} \mathbb{E}_{\mathbf{u}, \mathbf{v}} [\phi_E] &= \int d\mathbf{u} d\mathbf{v} \prod_i p(u_i^a) \sum_{\{s_i^a\}} \exp \left[\sqrt{L} s_i^a \sum_{\alpha, a} w_{\alpha} m_{\alpha}^a u_i^a \right] \prod_{\mu} p(v_{\mu}^a) \sum_{\{\tau_{\mu}^a\}} \exp \left[\sqrt{L} \tau_{\mu}^a \sum_{\alpha, a} w_{\alpha} \bar{m}_{\alpha}^a v_{\mu}^a \right] \\ &= \prod_i \left\{ \int \prod_{\alpha} du_i^a p(u_i^a) \sum_{\{s_i^a\}} \exp \left[\sqrt{L} s_i^a \sum_{\alpha, a} w_{\alpha} m_{\alpha}^a u_i^a \right] \right\} \times \end{aligned}$$

$$\begin{aligned}
& \prod_{\mu} \left\{ \int \prod_{\alpha} d v_{\mu}^{\alpha} p(v_{\mu}^{\alpha}) \sum_{\{\tau_{\mu}^{\alpha}\}} \exp \left[\sqrt{L} \tau_{\mu}^{\alpha} \sum_{\alpha, a} w_{\alpha} \tilde{m}_{\alpha}^a v_{\mu}^{\alpha} \right] \right\} \\
&= \left(\int d u p(u) \prod_a \sum_{\{s^a\}} \exp \left[\sqrt{L} s^a \sum_{\alpha} w_{\alpha} m_{\alpha}^a u^{\alpha} \right] \right) \left(\int d v p(v) \prod_a \sum_{\{\tau^a\}} \exp \left[\sqrt{L} \tau^a \sum_{\alpha} w_{\alpha} \tilde{m}_{\alpha}^a v^{\alpha} \right] \right) \\
&= \mathbb{E}_{\mathbf{u}} \left[2^n \prod_p \cosh \left(\sqrt{L} \sum_{\alpha} w_{\alpha} m_{\alpha}^p u^{\alpha} \right) \right]^{N_v} \mathbb{E}_{\mathbf{v}} \left[2^n \prod_p \cosh \left(\sqrt{L} \sum_{\alpha} w_{\alpha} \tilde{m}_{\alpha}^p v^{\alpha} \right) \right]^{N_h}
\end{aligned}$$

We can now explicit the scaling of the elements $u_i^{\alpha} \sim \tilde{u}_i^{\alpha} \sqrt{N_v}$ and $v_{\mu}^{\alpha} \sim \tilde{v}_{\mu}^{\alpha} \sqrt{N_h}$. By changing the integral, we obtain

$$\begin{aligned}
\mathbb{E}_{\mathbf{u}, \mathbf{v}} [Z^n] &= \int \prod_{\alpha, a} \frac{d m_{\alpha}^a d \tilde{m}_{\alpha}^a}{2\pi} \exp \left[-L \left(\sum_{\alpha, a} w_{\alpha} m_{\alpha}^a \tilde{m}_{\alpha}^a - \frac{1}{\sqrt{\kappa}} \mathbb{E}_{\mathbf{u}} \left[\log 2 \cosh \left(\kappa^{1/4} \sum_{\gamma} w_{\gamma} m_{\gamma}^a u^{\gamma} \right) \right] \right. \right. \\
&\quad \left. \left. - \sqrt{\kappa} \mathbb{E}_{\mathbf{v}} \left[\log 2 \cosh \left(\kappa^{-1/4} \sum_{\gamma} w_{\gamma} \tilde{m}_{\gamma}^a v^{\gamma} \right) \right] \right) \right]
\end{aligned}$$

from which we can obtain the free energy by assuming the replica symmetry and gather the terms that are linear in n .

References

- [1] Daniel J Amit, Hanoch Gutfreund, and Haim Sompolinsky. Storing infinite numbers of patterns in a spin-glass model of neural networks. *Physical Review Letters*, 55(14):1530, 1985.
- [2] Elizabeth Gardner and Bernard Derrida. Optimal storage properties of neural network models. *Journal of Physics A: Mathematical and general*, 21(1):271, 1988.
- [3] Marc Mézard and Thierry Mora. Constraint satisfaction problems and neural networks: A statistical physics perspective. *Journal of Physiology-Paris*, 103(1-2):107–113, 2009.
- [4] David L Donoho, Arian Maleki, and Andrea Montanari. Message-passing algorithms for compressed sensing. *Proceedings of the National Academy of Sciences*, 106(45):18914–18919, 2009.
- [5] Florent Krzakala, Marc Mézard, François Sausset, YF Sun, and Lenka Zdeborová. Statistical-physics-based reconstruction in compressed sensing. *Physical Review X*, 2(2):021005, 2012.
- [6] Hidetoshi Nishimori. *Statistical physics of spin glasses and information processing: an introduction*. Clarendon Press, 2001.
- [7] Hidetoshi Nishimori. Exact results and critical properties of the ising model with competing interactions. *Journal of Physics C: Solid State Physics*, 13(21):4071, 1980.
- [8] Yukito Iba. The nishimori line and bayesian statistics. *Journal of Physics A: Mathematical and General*, 32(21):3875, 1999.
- [9] Lenka Zdeborová and Florent Krzakala. Phase transitions in the coloring of random graphs. *Physical Review E*, 76(3):031131, 2007.
- [10] Aurelien Decelle, Florent Krzakala, Cristopher Moore, and Lenka Zdeborová. Inference and phase transitions in the detection of modules in sparse networks. *Physical Review Letters*, 107(6):065701, 2011.
- [11] Bruno Loureiro, Cédric Gerbelot, Hugo Cui, Sebastian Goldt, Florent Krzakala, Marc Mézard, and Lenka Zdeborová. Capturing the learning curves of generic features maps for realistic data sets with a teacher-student model. *arXiv preprint arXiv:2102.08127*, 2021.
- [12] Adriano Barra, Giuseppe Genovese, Peter Sollich, and Daniele Tantari. Phase transitions in restricted boltzmann machines with generic priors. *Physical Review E*, 96(4):042156, 2017.
- [13] Jérôme Tubiana and Rémi Monasson. Emergence of compositional representations in restricted boltzmann machines. *Physical review letters*, 118(13):138301, 2017.
- [14] Aurélien Decelle, Giancarlo Fissore, and Cyril Furtlehner. Thermodynamics of restricted boltzmann machines and related learning dynamics. *Journal of Statistical Physics*, 172(6):1576–1608, 2018.
- [15] Juan Carrasquilla and Roger G Melko. Machine learning phases of matter. *Nature Physics*, 13(5):431–434, 2017.
- [16] Frank Rosenblatt. The perceptron: a probabilistic model for information storage and organization in the brain. *Psychological review*, 65(6):386, 1958.
- [17] Christopher M Bishop. Pattern recognition. *Machine learning*, 128(9), 2006.
- [18] Yann LeCun, Yoshua Bengio, et al. Convolutional networks for images, speech, and time series. *The handbook of brain theory and neural networks*, 3361(10):1995, 1995.
- [19] Mark A Kramer. Nonlinear principal component analysis using autoassociative neural networks. *AICHE journal*, 37(2):233–243, 1991.
- [20] Alireza Makhzani, Jonathon Shlens, Navdeep Jaitly, Ian Goodfellow, and Brendan Frey. Adversarial autoencoders. *arXiv preprint arXiv:1511.05644*, 2015.
- [21] Pascal Vincent, Hugo Larochelle, Isabelle Lajoie, Yoshua Bengio, Pierre-Antoine Manzagol, and Léon Bottou. Stacked denoising autoencoders: Learning useful representations in a deep network with a local denoising criterion. *Journal of machine learning research*, 11(12), 2010.

- [22] Diederik P Kingma and Max Welling. Auto-encoding variational bayes. *arXiv preprint arXiv:1312.6114*, 2013.
- [23] Carl Doersch. Tutorial on variational autoencoders. *arXiv preprint arXiv:1606.05908*, 2016.
- [24] Diederik P Kingma and Max Welling. An introduction to variational autoencoders. *arXiv preprint arXiv:1906.02691*, 2019.
- [25] Ian Goodfellow, Jean Pouget-Abadie, Mehdi Mirza, Bing Xu, David Warde-Farley, Sherjil Ozair, Aaron Courville, and Yoshua Bengio. Generative adversarial nets. *Advances in neural information processing systems*, 27, 2014.
- [26] Elizabeth Gardner. The space of interactions in neural network models. *Journal of physics A: Mathematical and general*, 21(1):257, 1988.
- [27] Andreas Engel and Christian Van den Broeck. *Statistical mechanics of learning*. Cambridge University Press, 2001.
- [28] John J Hopfield. Neural networks and physical systems with emergent collective computational abilities. *Proceedings of the national academy of sciences*, 79(8):2554–2558, 1982.
- [29] Geoffrey E Hinton. Training products of experts by minimizing contrastive divergence. *Neural computation*, 14(8):1771–1800, 2002.
- [30] Aurélien Decelle, Cyril Furtlehner, and Beatriz Seoane. Equilibrium and non-equilibrium regimes in the learning of restricted boltzmann machines. *arXiv preprint arXiv:2105.13889*, 2021.
- [31] Timm Plefka. Convergence condition of the tap equation for the infinite-ranged ising spin glass model. *Journal of Physics A: Mathematical and general*, 15(6):1971, 1982.
- [32] Marylou Gabrié, Eric W Tramel, and Florent Krzakala. Training restricted boltzmann machines via the thouless-anderson-palmer free energy. *arXiv preprint arXiv:1506.02914*, 2015.
- [33] Moshir Harsh, Jérôme Tubiana, Simona Cocco, and Remi Monasson. ‘place-cell’ emergence and learning of invariant data with restricted boltzmann machines: breaking and dynamical restoration of continuous symmetries in the weight space. *Journal of Physics A: Mathematical and Theoretical*, 53(17):174002, 2020.
- [34] Adriano Barra, Giuseppe Genovese, Peter Sollich, and Daniele Tantari. Phase diagram of restricted boltzmann machines and generalized hopfield networks with arbitrary priors. *Physical Review E*, 97(2):022310, 2018.
- [35] Adriano Barra, Alberto Bernacchia, Enrica Santucci, and Pierluigi Contucci. On the equivalence of hopfield networks and boltzmann machines. *Neural Networks*, 34:1–9, 2012.
- [36] Marc Mézard. Mean-field message-passing equations in the hopfield model and its generalizations. *Physical Review E*, 95(2):022117, 2017.